YOKOHAMA CITY UNIVERSITY

DOCTORAL THESIS

Noise influence on spike activation in a Hindmarsh-Rose small-world neural network

---

Author:
Sun ZHE

Supervisor:
Prof. Ruggero MICHELETTO

Yokohama City University

in the

Micheletto Sensory Information Laboratory
Department of Materials System Science

acknowledgements I wish thank all those people that helped and supported me to learn knowledge and explore the unknown: my parents, my supervisor, and all of my friends.

Since I was a primary school student, I wanted to become a good scientist. I believe without my supervisor Professor Ruggero Micheletto, I will never achieve this dream.

I also would like to thank Professor Andrzej Cichocki and Professor Keiichi Kitajo in RIKEN Brain Science Institute, who have given me a lot of advice for my research.

I would like also to thank all of the help from the professors and researches in Yokohama City University and RIKEN Brain Science Institute.

I really appreciate Rotary-Yoneyama Memorial foundation, Donghua China-Japan Education and Cultural Exchange foundation, Nitori Scholarship foundation. I am so grateful they funded my Master course and Ph.D. course.

Chapter 1

Introduction

1.1 Reasons to study the brain

Without any doubt the brain is the most fabulous machine in the universe.

Animals have brains and we humans have brains. We actually *are* brains. All our activities and bodily functions are directed by the brain under control of the brain.

In the past human were thinking that science was a discipline of research separated from the science of the mind. We human, were convinced that not living things, like materialistic matter like physics, engineering, chemistry or biology, were fields that could be studied using science. However, there was the conviction that brain was a separate field of study.

Studying the brain was out of question. Brain was considered to be a mysterious entity, in which mind, consciousness and soul reside. At the beginning of the century, many scientists in the life science field started to investigate on the brain using simple tools, first doing post-mortem examinations in animals and humans, and later with modernization studying the brain more systematically.

It was soon discovered that brain shows a lot of electrical activity and the sole active element in the brain is the neuron, a specialized cell. This cell, that I will describe later, is a simple element that essentially does only one simple thing: it gives a quick electric impulse, called *spike*, or *action potential*. I will describe this functions later in details. However, our brain is simply a complex connection of a great number of neurons.

Currently science have no idea how all our creativity, our consciousness and our ability to think and change the world around us, are realized simply by connecting many neurons together. We can imagine that one day we will be able to understand how the brain works, when that day will arrive, we will be able to construct artificial brains. This will give an enormous impulse to human technology and human society as a whole.

Brain is not a magic box, something that we do not have the scientific means to study. Brain is a machine, a computational machine. It is made by connected neurons, and for small animals with small brains, we even know almost perfectly the connections configuration. Brain give small animals perfect control on their bodies and functions. A bee for example, can solve very difficult problems, like flying from one place to the other, arriving on km away flower filed, land exactly to a flower, take the pollen, lift off and find the way fly back home.

A bee is even able to communicate to other bees the position of the field, using complex body language communication. All of this, plus many other things, are realized by the very small brain of the insect, that have less than one million neurons. Take in account that a neuron can emit its spikes at maximum rate of 200 Hz, whereas our best computers cannot yet land a plane automatically. We need a brain to do that.

Even if brains are so slow and so simple, they give animals full control of their bodies, they allow the solutions of very complex problems and the realization of very structured societies (consider the societies of Ants, that have a brain with only 250.000 neurons). Brains also have huge memory, consider for example the enormous amount of things that we adult human know, but also small ants and small animals, are able to memorize a lot of things, with minimal brains sizes.

What are currently the facts about the brain ? We will show later that we know exactly how one neuron works. We have currently mathematical models that can emulate almost perfectly the electrical functioning of a single neuron.

Even if brains are simply many neurons connected in an intricate way, we have no theory about how the brain works. If we could understand that, it will be for sure the most important discovery in human history.

One of the most important motivation to study the brain, is not only the possible technological applications that we can achieve with artificial-brain science, but by the fact that up to few years ago brains were basically studied solely by life-science researchers. These scientists studied the brain from the functionality point of view, trying to understand what are the inner functions a brain, but leaving aside the more complex theoretical and mathematical reproductions of these functions. For this goal, the goal to achieve understanding and reproduce artificially brain functions, scientists like physicists, mathematicians and engineers are more qualified, because they are more accustom to construct and simulate physical systems and machines.

In other words, the brain is a computational machine, so we need also physicists, mathematicians and engineers to understand it and reveal its secrets. G. Neves (Nature Reviews Neuroscience, 9, 65-75, 2008) states in a paper on Synaptic plasticity that we do not know yet how networks of neurons work. In particular in his study they concentrate on the how networks encode and represent memory. Even the most simple memory element, the binary minimal entity *yes* or *no* or 0/1 case, is not clear how it is represented in our brain. For example we may have decide if to go to the cinema tomorrow or not. Once this decision has been taken, the information *yes* I will go, or *no* I will not will be stored somewhere in our brain. Even this very small information bit is not known how it is stored by the brain.

Buonomaro [11] in Nature Reviews in 2009 have shown that we do not have yet a computational framework for the brain. This theoretical background remains elusive and we have very few insight on how to proceed.

Some authors like Karl Friston, in Nature Reviews Neuroscience, vol 11, 2010, put forward the problem of a unified brain theory. We need a paradigm that can help us to understand and decode the brain functioning and unfortunately we do not have that yet.

The study of brain principles is at the beginning of its history. Any small incremental contribution to the mathematical and theoretical investigation on the brain could be a discovery of paramount importance. There is a great potential for fundamental discovery in the study of the finding of how the brain works and how we could cure it. Life-science brain research is also concerned on why certain functions are working in a certain way and how this is inserted in the big picture of an organism.

However, physicists, mathematicians and engineering have a different perspective. The final goal of these researchers is to reproduce the functions of the brain on machines. The intermediate goal is to establish a theoretical framework, that is currently almost completely missing. We want to understand what is the mathematics behind brain working, and what are the algorithms running in the brain. Brain for us is a *computational machine*, so we need computational theory understanding to solve the mystery of the brain functioning. The ultimate goal of this is to implement brain algorithms on machinery, networks and computers in order, not only to understand better how we work, but also to realize new intelligent devices, much better, faster and reliable than us.

Currently brain research, from this latter point of view, is beginning to be

found on journals like Physical Review E, Physica A, Physical Review Letters, Journal of Physics A to cite a few prominent Physics journals. Other physic related journals that publish on brain and cognitive research are Institute of Physics Chaos, PLoS one and of course more generalist an highly cited magazines like Science or Nature

1.2 The neuron and brain

Through human sense (vision, auditory, touch sense, taste, smell, equilibrium) brain gets external information and process the information. The functioning of the brain is very complex, the basic unit is neuron. The human brain is made up of billions of neurons. Each neuron has a cell body, an axon, synapses and many dendrites.

Neurons have a difference in voltage between the inside of the cell and its exterior environment. Each neuron maintains a potential difference across its membrane inside is about –70 mV relative to outside. This flux of ions creates the a difference in the concentration of certain ions, and therefore in voltage, between its outside and inside. For one neuron system, the most important ions are potassium (K^+), sodium (Na^+), chlorine (Cl^-), and calcium (Ca^{2+}), and each ion channel accepts only one of these ion species.

As in figure 1.1, Na^+ and Cl^- concentrations are higher outside; K^+ concentration is higher inside When the neuron is stimulated by chemical or physical elements, such as receiving a neurotransmitter (chemical synapse) or electrical synapse (gap junction), some of Na^+ channels will open, allowing positively charged Na^+ ions to go inside the neuron. This Na^+ invasion depolarizes the neuron membrane potential as in the figure 1.3. If this depolarization continues and the potential surpass a specific threshold value, an action potential (spike) will be generated. Much more Na^+ ion channels suddenly open, allowing the neuron to flood with positively charged Na+ ions, so the membrane potential will generate a peak. We call the electrical pulse during this period *action potential* or *spike*. Action potential is the basis of information transfer and processing between neurons in the brain.

1.3 Neuron Model

In 1952, in order to develop an mathematical model to describe how a neuron's membrane potential evolves and the variety of action potentials (spikes), scientist A.L. Hodgkin and A.F. Huxley observed the action potentials in the

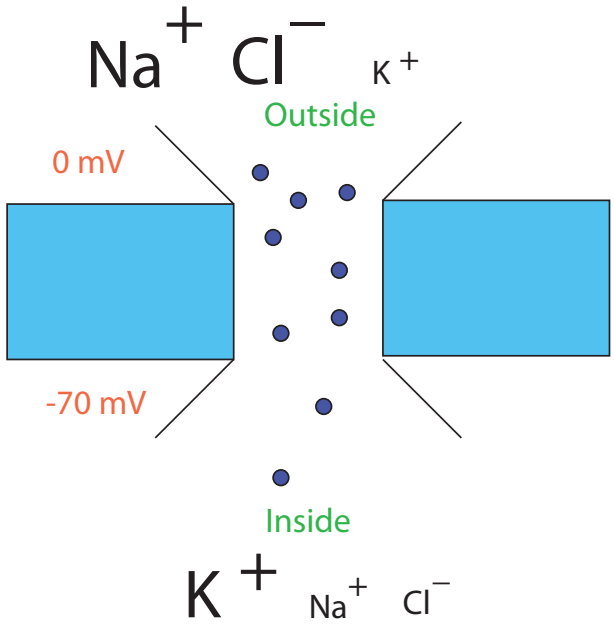

FIGURE 1.1: This movement of ions will change the membrane potential.

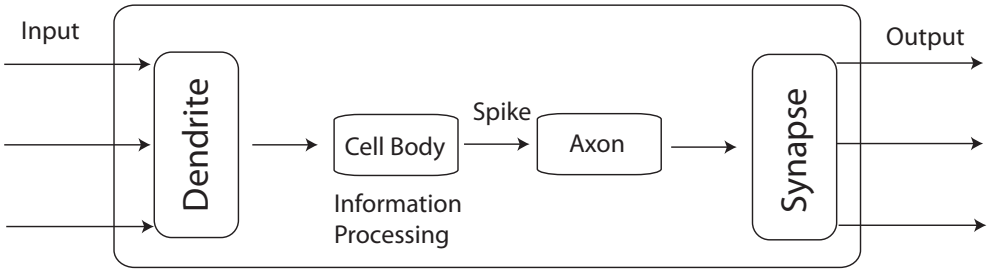

FIGURE 1.2: Function model of a neuron

squid's giant axon and developed the so called Hodgkin-Huxley equation. The equation is described as following:

$$
\begin{aligned}
&I = Cdv/dt + \bar{g}_{Na}m^3h(V - V_{Na}) + \bar{g}_k n^4(V - V_k) + \bar{g}_L(V - V_L),\\
&dm/dt = (S_m(V) - m)/T_m(V),\\
&dh/dt = (S_h(V) - h)/T_h(V),\\
&dn/dt = (S_n(V) - n)/T_n(V).\\
&C = 1\mu F/cm^2, \qquad \bar{g}_{Na} = 120.0mS/cm^2, \qquad \bar{g}_k = 36.0mS/cm^2\\
&\bar{g}_L = 0.3mS/cm^2, \qquad V_{Na} = 55.0mV, \qquad V_K = 55.0mV,\\
&V_L = -49.387mV
\end{aligned}
\tag{1.1}
$$

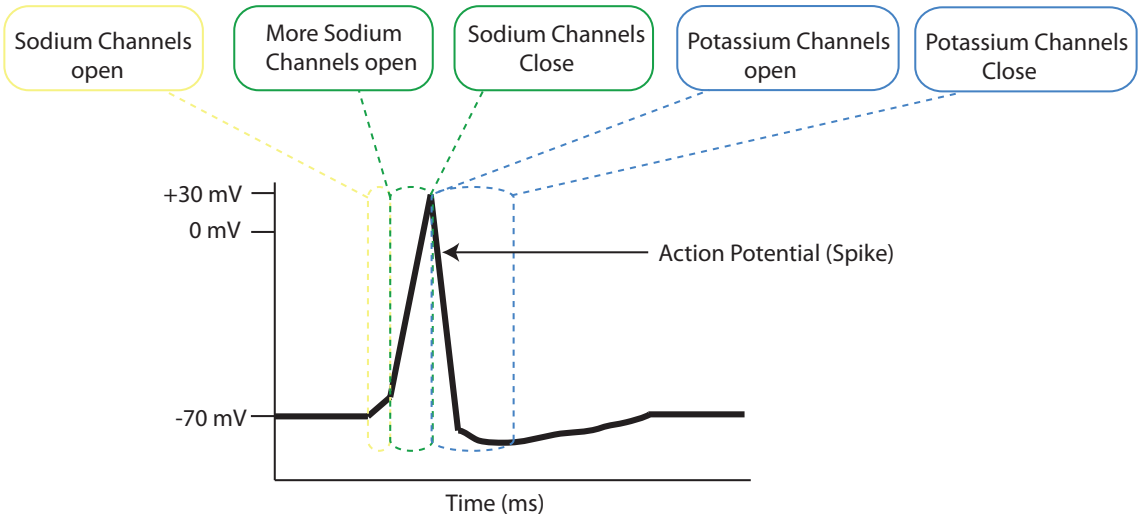

FIGURE 1.3: In this diagram of an action potential, you can see the membrane potential spike that peaks around $+30mv$ (as you can see, this neuron's resting potential is a little higher than the usual $-70mV$). This kind of electrical pulse is called action potential (spike)

In this equation:
V is membrane potential;
m is Na^+ activation ($0 < m < 1$);
n is the K^+ activation ($0 < n < 1$);
h is the Na^+ inactivation ($0 < h < 1$);
t is time (ms);
I is current ($\mu A/cm^3$).

As in equation 1.1, Hodgkin-Huxley model has four variables with four equations. g_{Na} and g_K are the electrical conductance of the Na^+ and K^+, parameters n, m, h are the gating unit variables to describe the probabilities of opening ion gate. Hodgkin-Huxley model succeed for the explanation of action potential generation in a neuron.
In 1982, depend on the action potentials of snail neurons, Hindmarsh and Rose constructed the Hindarmarsh-Rose neuron model. Now, this model is used to simulate the dynamics of membrane potential observed in one neuron. The system is characterized by three independent variables that represent the membrane potential and the two ion channel currents. The single neuron model is described by the following differential equation:

$$\begin{cases} \dot{x} = y - ax^3 + bx^2 - z + I \\ \dot{y} = c - dx^2 - y \\ \dot{z} = r[s(x - \chi) - z] \end{cases} \tag{1.2}$$

In this equation, x is time dependent and represents the membrane potential, whereas y and z are often called the spiking and bursting variables, respectively[18]. Those variables are all expressed in arbitrary units and do not have a direct translation in biologically realistic parameters[27]. And in the following figure, it shows the simulation of membrane potential phenomenon in one burst spiking neuron.

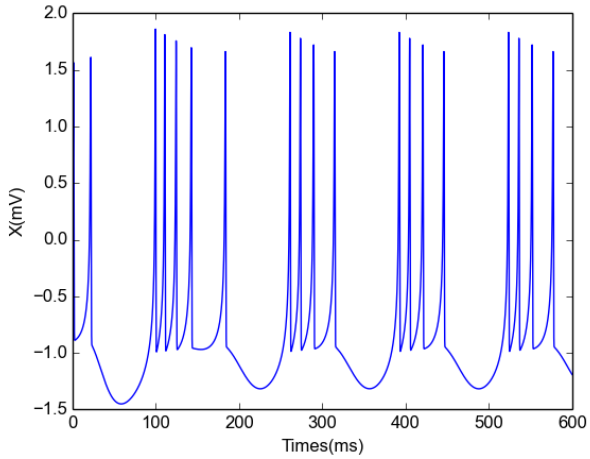

FIGURE 1.4: Simulation of Hindmarsh-Rose model and it shows burst spiking activity of one neuron.

Another very efficient model for neuron dynamics simulating is the model developed by Izhikevich[30]:

$$\frac{dv}{dt} = h_1 v^2 + h_2 v + h_3 - u + I^{ext} + I^{syn}, \tag{1.3}$$

$$\frac{du}{dt} = a(bv - u). \tag{1.4}$$

After the neuron emits a spike, action potential will reset:

$$if \quad v \geq 30mV, \quad then \quad \begin{cases} v \leftarrow c \\ u \leftarrow u + d. \end{cases} \tag{1.5}$$

This is a reduced, bi-dimensional canonical model that reproduces most prominent behaviour of mammal cortex neurons[13, 61]. The variable u is the membrane recovery variable that represents the activation of K^+ channels or inactivation of Na^+ or both the phenomena. Parameter a, b, c, d are used for regulating the types of neurons. In fact, a represents the time scale of variable u to recover from a firing, and b determines its sensitivity to the fluctuations of variable v. Moreover, c is the after-spike reset value of the membrane potential v and, in the same fashion, $u + d$ is the value that the

recovery variable u resets immediately after-spike. In the equation, I^{ext} denotes a generalized external stimulus and I^{syn} is the synaptic current from a connected pre-synaptic neuron.

In chapter 1, I studied a two coupled-neurons system, as an element and building block of larger networks. Differently from literature studies, we simulated two isolated neurons coupled by finely controlled connection strength parameter w to elucidate its discontinuous effect on the system dynamics (Stich and Verlade used a dynamically changing w whereas Wei et al. tested w in few discrete points). Three general classes of neurons were simulated: bursting, non-bursting with frequency adaptation and frequency acceleration properties: a chattering (CH, bursting) neuron, a regular spiking (RS, frequency adaptation) neuron and a fast spiking (FS, frequency acceleration) neuron. To account for the representation of a brain system, noise and heterogeneity are incorporated in the equations in a realistic fashion.

In chapter 2, we emulated a triggering event in the brain through a single active neuron that we call *initiator* x_o and, in controlled noise conditions, we study the flow of spike activity along the network to evaluate the role of noise amplitude on the signal propagation. We elucidate in a quantitative manner the role of noise and we found for the first time a linear relationship between the amplitude expressed in decibel and the delay interval between initiator x_o first spike and the network activation.

Chapter 2

Non-linear and threshold effects of synaptic connectivity on the correlation parameter of a system of two coupled neurons.

2.1 Coupled Neurons and synaptic connectivity

The analysis of human brain's neural network behavior is very important for the development of next generation intelligent devices[38, 80]. However, practical applications on how to realize pattern recognition or natural language processing is still a quite difficult problem[49, 12, 42, 25, 74] where the understanding of actual brain mechanism may be groundbreaking. Key to realize progress is the quantitative understanding of the fundamental mechanism related to learning and memory function in our brain, that is to shed light on the so called *synaptic plasticity*, the variation of connection strength between neurons[44]. In this process, temporal relation between spike trains can alter the connection strength between neurons and it is the crucial mechanism for learning and memory[68, 69, 3].

Even if the behaviour of a single neuron is known and its representation with analytical functions possible, the study of two or more connected neurons is difficult because of the extreme non-linearity of neuronal models and the lack of proper tools. The study of complex networks of neurons is baffling despite great efforts because we do not have an established theory on how the Brain encodes, transmits and decodes information. Inspired by the work of Wei, Perez and Cerdeira[78], and the more recent and prominent study of Stich and Velarde[70], the main motivation of this study is to simplify as much as possible the problem and study a two coupled-neurons system, as

an element and building block of larger networks. Differently from literature studies, we simulated two isolated neurons coupled by finely controlled connection strength parameter w to elucidate its discontinuous effect on the system dynamics (Stich and Verlade used a dynamically changing w whereas Wei et al. tested w in few discrete points). Three general classes of neurons were simulated: bursting, non-bursting with frequency adaptation and frequency acceleration properties: a chattering (CH, bursting) neuron, a regular spiking (RS, frequency adaptation) neuron and a fast spiking (FS, frequency acceleration) neuron. To account for the representation of a brain system, noise and heterogeneity are incorporated in the equations in a realistic fashion.

2.2 Model

A very efficient and widely applicable simulation method is the Izhikevich model[35]:

$$\frac{dv}{dt} = h_1 v^2 + h_2 v + h_3 - u + I^{ext} + I^{syn}, \tag{2.1}$$

$$\frac{du}{dt} = a(bv - u). \tag{2.2}$$

After the neuron emits a spike, action potential will reset:

$$if \quad v \geq 30mV, \quad then \quad \begin{cases} v \leftarrow c \\ u \leftarrow u + d. \end{cases} \tag{2.3}$$

This is a reduced, bi-dimensional canonical model that reproduces most prominent behaviour of mammal cortex neurons[13, 61]. In this equation, $h_1 = 0.04$, $h_2 = 5$ and $h_3 = 140$ are constants scaled by Izhikevich in order to have the time t in milliseconds and the voltage v in millivolts. The variable u is the membrane recovery variable that represents the activation of K^+ channels or inactivation of Na^+ or both the phenomena. Parameter a, b, c, d are used for regulating the types of neurons. In fact, a represents the time scale of variable u to recover from a firing, and b determines its sensitivity to the fluctuations of variable v. Moreover, c is the after-spike reset value of the membrane potential v and, in the same fashion, $u + d$ is the value that the recovery variable u resets immediately after-spike[35]. In the equation, I^{ext} denotes a generalized external stimulus and I^{syn} is the synaptic current from a connected pre-synaptic neuron.

In this framework, the analytical expression of two neuron connected with a strength w is given by the solution of this system of differential equations:

$$\begin{cases} \dot{v}_m = h_1 {v_m}^2 + h_2 v_m + h_3 - u_m + {I_m}^{ext} \\ \dot{v}_n = h_1 {v_n}^2 + h_2 v_n + h_3 - u_n + {I_n}^{ext} + w * (v_m - v_n), \end{cases} \tag{2.4}$$

where we indicated with the index m the pre-synaptic and n the post-synaptic neurons (the signal transfers from pre-synaptic neuron to post-synaptic neuron). We would like to have completely analytical expression relating the post-synaptic membrane potential to the pre-synaptic one in function of the connection strength w. However, the study of this is difficult because of the non-derivable nature of the threshold in equation (2.3), so numerical simulation is adopted. Figures 2.1, 2.2, 2.3 show the spike train of three classes of neurons simulated with the model described in details below. The so-called *chattering* (CH) neurons exist in superficial layers of the cortex and generate synchronous oscillations in the visual cortex[24]. They are excitatory neurons and generate repetitive bursts and short-duration spikes. The *regular spiking* (RS) neurons are typically spiny pyramidal cells which widely exist in the brain[41]. These are excitatory neurons and characterized by spike-frequency adaptation, that is the slow increase in inter-spike interval at constant stimulation.

The third class used is the so-called *fast spiking* (FS) that have similar high firing rates, but show the opposite phenomena of spike-frequency acceleration. Some cortical inhibitory inter-neurons belong to this type and are important for the generation of gamma waves in the brain. In general FS neurons and RS neurons exhibit no bursts and inter-spike interval of RS neurons are broader than CH and FS neurons[55, 23, 33] (for other details see Izhikevich 2007[30]).

We used two configurations to couple the two neurons. In the first configuration, to induce spiking the pre-synaptic neuron m is excited by a constant current I^{ext}[9]. We want to study the bare effect of stimulation, so post-synaptic neuron is not stimulated, but reacts solely to the pre-synaptic signals (configuration A). In another test (configuration B), both of the two neurons are connected to an external stimulus. These two configurations exist in realistic neural system. A correlation parameter ρ (introduced later in equation (2.9)) was used to estimate the correlation between the spike train of the two neurons in function of connection strength w.

	a	b	c	d
CH	0.02	0.2	-50	2
RS	0.02	0.2	-65	8
FS	0.1	0.2	-65	2

TABLE 2.1: Values of parameters a, b, c, d. These four parameters are used for determining the types of neurons.

The already mentioned figures 2.1, 2.2, 2.3 show the resulting action potential variable v of three types of neurons CH, RS, FS over time t. Simulations have been performed with the model described in equations (2.1), (2.2) and (2.3) with $I_{ext} = 8mA$ where values of the parameters a, b, c, d are defined as in Table 2.1. No other input signals, internal or external noises are introduced. T

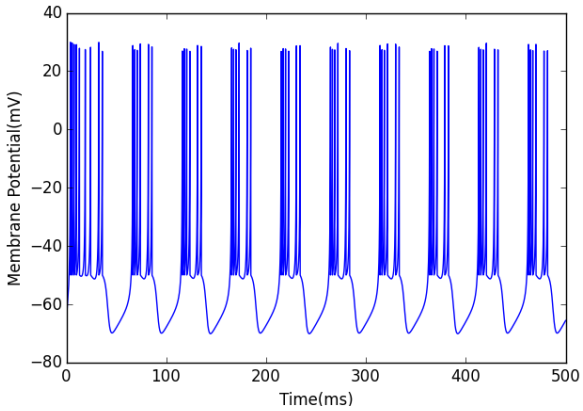

FIGURE 2.1: Spike train of a CH neuron, the external stimulus I^{ext} was fixed at $8mA$. The value of the membrane potential is calculated every 0.01 ms for 50000 data points.

.

Neuron m and neuron n are coupled by a single electrical synapse that mediates the two action potentials $v_m(t)$ and $v_n(t)$ (see figure 2.5). The connection strength w ranges from 0.0 to 1.0. To avoid artifacts due to the representation of identical neurons and the systematic summation of numerical errors, we introduced heterogeneity and a small level of noise, elements that are present in actual biological systems. Heterogeneity was introduced by defining CH and RS neurons with a and b parameter fixed accordingly to table (2.1) and variable parameters c_m and d_m. Those are centered in table (2.1)'s c and d and spread randomly accordingly to the formulas $c_m = c+15r_m^2$ and $d_m = 8 - 6r_m^2$, r_m is a uniform-distributed random variable on the interval [0,1] (Izhikevich, 2003[35]). In the case of FS neurons, we defined $a_m = a + 0.08r_m$ and $b_m = b - 0.05r_m$ and c and d are constant accordingly

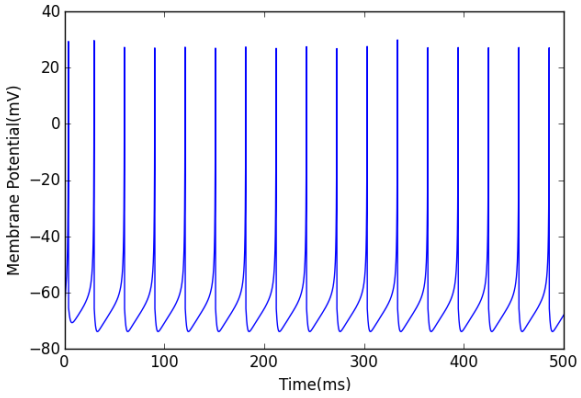

FIGURE 2.2: Spike profile for a RS neuron, the external stimulus I^{ext} is 8mA, time step 0.01 ms and there are 50000 points in the graph

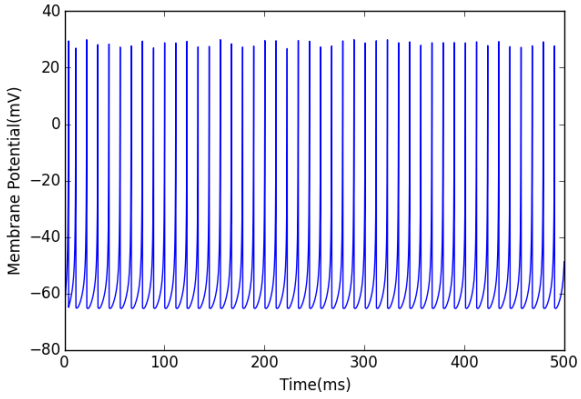

FIGURE 2.3: A plot of the action potential of the FS neuron described in the text. The external stimulus I^{ext} is fixed at 8mA. Time interval is 0.01 ms for a total of 50000 data points.

again to table (2.1). Concerning the external noise term, we consider that in a real biological system, adjacent spiking neurons will generate a noise that has the statistical distribution of the sum of each of those neurons. The central limit theorem states that the sum of a great number of arbitrarily distributed event tends to a Gaussian distribution, so the noise in our simulations is distributed in the same way (Bennet, 2004[8]).

Firstly, we generated a Gaussian distributed random variable $X \sim N(\mu, \sigma^2)$. Here X is generated internally by a standard numerical library (python *numpy*), μ is the mean value around which the Gaussian is centered and σ is the corresponding standard deviation.

The differential equations are integrated with Euler method and the index i represents the i_{th} integration loop. For each simulation conditions a trial running is done to evaluate the average amplitude of the action potential A,

this value is then used as a constant parameter in the actual tests,

$$A = \frac{\Sigma_i v_i}{N}. \tag{2.5}$$

Accordingly to literature[16, 86], a reasonable value for noise level in real brains is about 20dB, so SNR(signal-to-noise ratio) was defined as $10\log_{10}(\frac{A}{A_{noise}})^2$. The SNR was kept at 20 dB, so A_{noise} is

$$\begin{aligned} A_{noise}^2 &= \frac{A^2}{10^{\frac{SNR}{10}}}, \\ \varepsilon_i &= A_{noise} X_i, \end{aligned} \tag{2.6}$$

where ε_i is the noise variable calculated at each integration loop. In our experiment, we used δt to estimate one step of the time interval. Equation (2.1) becomes:

$$v_{i+1} = v_i + (h_1 v_i^2 + h_2 v_i + h_3 - u_i + I_i^{ext} + I_i^{syn} + \epsilon_i)\delta t. \tag{2.7}$$

To avoid artifacts due to unrealistic instantaneous transfer of information, a fixed delay τ between two neurons interaction was introduced[39, 20, 28]. The time delay in mammalian neocortex is estimated by several biological experiments[72, 71], here the constant delay was fixed to $\tau = 0.01\ ms$[32]. We also fixed the single integration step (index i) δt as 0.01 ms in our Euler integration method. This will suffice to avoid artifacts and represent existent neuronal delay in a certain amount.

The equations governing the system of two neurons are described as the following:

$$\begin{cases} \dot{v(t)}_m = h_1 v_m(t)^2 + h_2 v_m(t) + h_3 - u_m(t) + I^{ext}(t) + \varepsilon_m(t) \\ \dot{v(t)}_n = h_1 v_n(t)^2 + h_2 v_n(t) + h_3 - u_n(t) + I^{ext}(t) + w * (v_m(t-\tau) - v_n(t)) + \varepsilon_n(t). \end{cases} \tag{2.8}$$

The term $w * (v_m(t-\tau) - v_n(t))$ represents the synaptic current for the post-synaptic neuron n with the information coming from the pre-synaptic neuron m retarded by a delay τ. The coefficient w is called here *connection strength* and ranges from zero (system decoupled) and one (a perfectly coupled system)[31]. The expressions relative to the recovery variable u and the threshold behavior are calculated accordingly to above equations (2.2) and (2.3) .

Synchronization and phase locking of the system was estimated by the correlation coefficients ρ with the following equations:

$$\rho = \frac{Cov(S_m, S_n)}{\sqrt{Var(S_m)Var(S_n)}}. \tag{2.9}$$

In this equation, Cov is the covariance between the vectors S_m and S_n and Var is the variance relative to the same vectors. To suppress sub-threshold activity from the correlation calculation, S is an one-dimension vector which stores over-thresholds intervals counts over a time-based slider window.

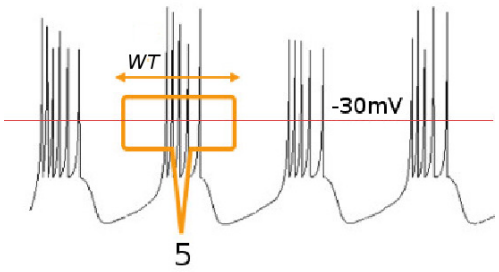

FIGURE 2.4: An exemplification of the method used to remove baseline values from correlation: a sliding window of duration WT is shifted along time. For every time step in which the action potential is over a threshold ($-30mV$), the counter for that window is increased of one unit. An array S is filled with integers that counts the time intervals in which the membrane potential was over the threshold, this happens for each time windows and then the window is shifted to the next adjacent position. The red box indicates the window range and the number 5 is just an example that coincide with the number of spikes visible. Note that, depending of the time step duration, actual count may differ from the spike count. In our study the window width is fixed to 3 $msec$ and time step to 0.1msec.

If Δ is the duration of the window (in figure 2.4, $\Delta = WT$), T is the length of a experiment[17], the spike train of membrane potential v is converted to the following binary data train MP:

$$MP(t) = \begin{cases} 1 & if \quad v(t) \geq -30mV \\ 0 & if \quad v(t) < -30mV. \end{cases} \tag{2.10}$$

The threshold was fixed as $-30\ mV$ to eliminate any sub-threshold activity in the correlation calculation. Any value over $-50mV$ or less than $20mV$, for example, could have been a good choice too; this particular threshold value was chosen in order to have an accurate representation of the spike

FIGURE 2.5: The two configurations used in our simulations. In panel (a) the pre-synaptic neuron m receives the external stimulus of $I_m = 8\ mA$. In panel (b) both the neurons receive an identical stimulus of $I = 8\ mA$. The synaptic current from neuron m is mediated by the connection strength parameter w.

event with our type of neurons. See figures 2.1, 2.2 and 2.3 for the exact spike profiles of them, see also figure 2.4 for a sketch of the method. According to the above, we determine the counts from time t_0 to $t + \Delta$. Then the time windows is shifted along the time axis and the counts are stored into the vector S as below:

$$\begin{aligned} &S(t) = \Sigma_t^{t+\Delta} MP(t), \\ &t \in \{\Delta, 2\Delta, 3\Delta..., T - \Delta\}. \end{aligned} \tag{2.11}$$

In this formula, Δ is the length of time windows and T is the length of simulation time, Δ is fixed as 3 ms in all our tests.

2.3 Results and discussion

We used two configurations to couple the two neurons. As shown in figure 2.5(a) and figure 2.5(b), in Configuration A neuron m has an external stimulus that forces it to spike regularly, neuron n spike trains are due solely to the stimulation received from m. In Configuration B instead, both of two neurons receive external stimuli. This configuration is used to test if effects observed in A are due to neuron m drive, or instead due to other implicit characteristics of neuron n.

First of all, we observed how the action potential changed when the connection strength w between the neurons is varied in Configuration A. In figure 2.6, we simulated two CH neurons and varied the connection strength w accordingly to configuration A. At first, low values of w do not induce spiking activity on n until values of about $w = 0.15$. Beyond this n generates spikes and the correlation of the system increases until the two neurons reach

very high synchronization. At values higher than $w = 0.45$, neuron m is giving the pace to its coupled n neuron that reaches locking, with correlation ρ of about 0.8. Even if this is the most simple network realizable, we can say that m acts as a sort of *pacemaker* of the system.

Interestingly, lag-synchronization is noticeable in the third plot of figure 2.6, where the two spikes trains appear to be locked, but with a shift in time (lag) that keeps the overall correlation coefficient low ($\rho = 0.156$). This fact is important[62, 10], however here we do not want to investigate on lag synchronization for reason of uniformity and clarity in respect to the correlation and connection strength dependence.

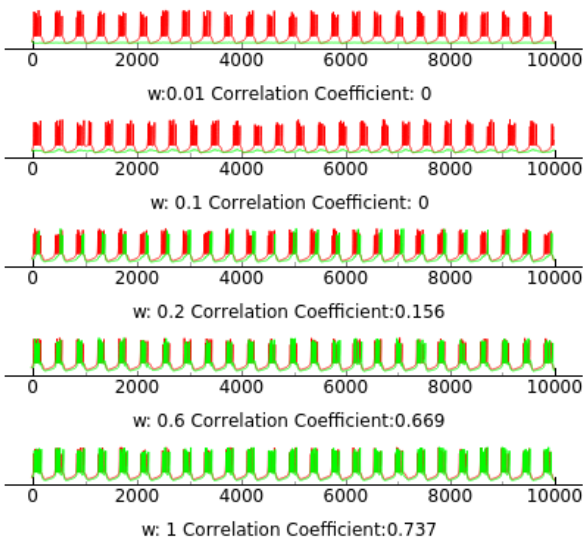

FIGURE 2.6: The figure shows spike trains of two coupled CH neurons. Only the pre-synaptic neuron is connected to an external stimulus of $I = 8$ mA. When w is increased, neuron n starts to generate spikes. The two neurons reveal very high synchronization when w reaches a maximum value.

From the dynamical system point of view, this means that for small w the pulses that neuron n receives from m, act as perturbation, too small in amplitude to alter the state variables of the neuron that remains around in its equilibrium point at $-65mV$. This is represented in the phase diagram of figure 2.7(a) where v_m potential is seen to range from $-60mV$ to $+20mV$ flat against an almost constant v_n that drift around few mV interval. When w grows over a certain threshold, these perturbations raise in amplitude until the equilibrium is broken and spiking begins. Moreover, the phase diagram of figure 2.7(d) shows a bifurcated shape for $\rho = 0.74$ indicating that the phases are locked at two different states in the two neurons (neuron n spikes

when m is about $-50mV$, whereas m spike seems to cover a wider span of n potentials, ranging from $-70\ mV$ to -40 mV).

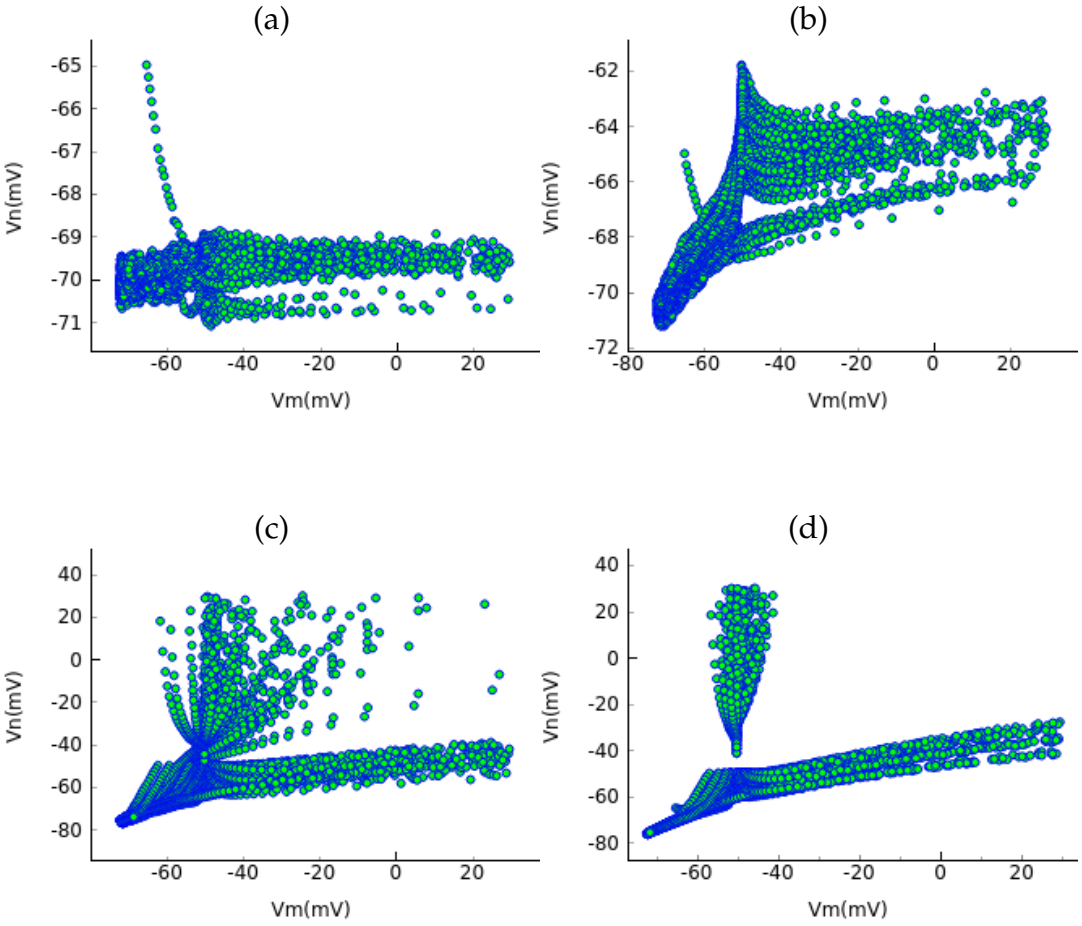

FIGURE 2.7: Strong non-linearity in w observed in the two neurons phase diagram. In this group of figures, the vertical axis is the action potential of the post-synaptic neuron n and the horizontal axis that of the pre-synaptic m, both the neurons are of type CH. In these simulations only neuron m is connected to the external stimulus to induce regular beating. In (a) the connection parameter w is very low ($w = 0.01$), in (b) ten times bigger ($w = 0.1$). Nevertheless in these two plots, the two neurons are not synchronized, their correlation coefficient ρ is negligible. In panel (c) and (d) the activity of the pre-synaptic neuron induce the other to spike in levels of synchronization proportional to w. In (c) $w = 0.6$ and $\rho = 0.66$, in (d) the connection is maximum at $w = 1.0$ and the correlation reaches $\rho = 0.74$.

Most interestingly, the behaviours observed indicate a strongly non-linear dependence of correlation against connection strength. In other words there

is not a linear or smooth transition to the two neurons system synchronization, the profile of ρ against w shown in figure 2.8 reveals a net threshold behaviour that is reproduced at different values for all types of neurons tested.

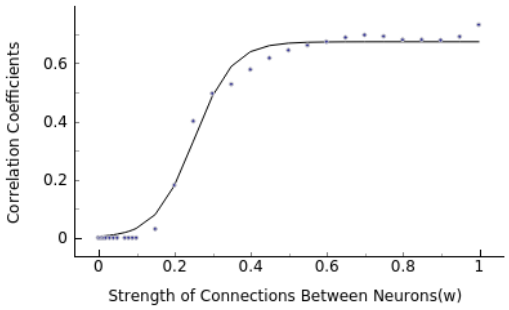

FIGURE 2.8: An example of dependence between correlation ρ and connection strength w between neuron m and n. A clear threshold and plateau behaviour is noticeable in most cases (this plot represent the interaction of two Chattering neurons (CH-CH system), the post-synaptic one has no external input). The dots are the correlation coefficients data, a sigmoid function is fitted along them to emphasize the non-linear, step-like behaviour.

Our simulations show that the electrical voltage coupling factor w dependence is non-linear and discontinuous, as shown for example shown later in figure 2.15 (a) where several neurons types exhibit abrupt rise in correlation with increased coupling value w. Nevertheless, data can be fitted with a sigmoid with three degree of freedom represented by three parameters α, β and w_0 in the function:

$$\Sigma(w) = \frac{\alpha}{1 + \exp^{-\beta(w-w_0)}}. \tag{2.12}$$

where w_0 represents the center of the sigmoid, in other words it represents the position of the threshold, whereas α and β represent the height and sharpness of the curve respectively. In table 2.2 we summarize the fitting parameter for all cases discussed.

The inter-spike interval (ISI) is key to several models of information coding in the nervous system[88] and can be used in a method to reconstruct the system dynamics[64]. The non-linear dependence of w on synchronization is reflected on a similar strong non-linearity in the inter-spike dynamics. We record the inter-spike interval mean μ_{ISI} and standard deviation σ_{ISI} for the system for the two different configurations. Using vector PT to record the spiking time of the post-synaptic neuron, fixing the spiking time index as j,

	α^A	w_0^A	α^B	w_0^B
CH-CH	0.67	0.25	0.90	-0.01
RS-RS	0.65	0.68	0.97	-0.07
FS-FS	0.75	0.86	0.95	0.037
CH-FS	0.70	0.30	0.87	0.26
CH-RS	0.58	0.24	0.64	0.21
FS-RS	0.25	0.85	0.29	0.62
FS-CH	0.21	0.85	0.77	0.57
RS-CH	0.79	0.65	0.82	0.16
RS-FS	0.77	0.63	1.03	0.44

TABLE 2.2: The fitting parameters α and w_0 for the sigmoid interpolation of the correlation function ρ versus connection strength w for various neuron types combinations (see CH-CH example in figure 2.8). Interpolation has been done with formula (2.12), α represents the height of the sigmoid plateau, and w_0 the center of the curve. The apex A or B of the parameters represent the two connection configurations in figure 2.5.

then the inter-spike element ISI_j can be represented as follows:

$$ISI_j \in \{PT(j+1) - PT(j) \mid j \in (1, 2...J-1)\}, \tag{2.13}$$

here J is the total number of spikes. According to the array of inter-spike intervals ISI, we calculated the mean μ_{ISI} and standard deviation σ_{ISI} as follows:

$$\begin{aligned} \mu_{ISI} &= \frac{\Sigma_1^j ISI_j}{j}, \\ \sigma_{ISI} &= \sqrt{\frac{\Sigma_1^j (ISI_j^2 - \mu_{ISI}^2)}{j}}. \end{aligned} \tag{2.14}$$

We show in figure 2.9 and 2.10 the average μ_{ISI} and the standard deviation σ_{ISI} of the post-synaptic inter-spike interval. All possible neurons types and configurations were examined. In the neurons of configuration A (Fig 5(a)), inter-spike activity is absent for low values of w (for clarity in the plot ISI value is set to zero), then begins at around $w = 0.1$ for most cases. The results also show higher values about $w = 0.4$ or $w = 0.5$ in the cases of RS-RS or FS-FS respectively. After the initial spiking, in all cases the average inter-spike interval decreases and converges to the 2-4 $msec$ range. This means that the spiking rates and the spiking intervals of post-synaptic neuron trend to a stable plateau. Interspike intervals become almost independent to the connection strength between the two neurons.

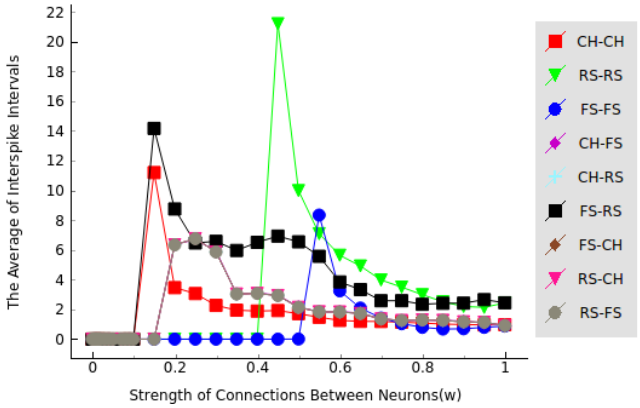

FIGURE 2.9: The y-axis show the average inter-spike interval μ_{Is} of the post-synaptic neuron n, the connection between the two neurons is configured as in figure 2.5(a), no external excitation for post-synaptic neuron. And each configuration shown is the average of 10 experiments, inter-spike variability is in the order of 20%. The figure show that RS neuron and FS neuron need more connection strength to spike compared to other types of neurons. The inter-spike interval was measured in ms. For low values of w, the post-synaptic neuron do not spike (interspike interval is infinite). For reason of clarity, we set the ISI value as zero in these cases.

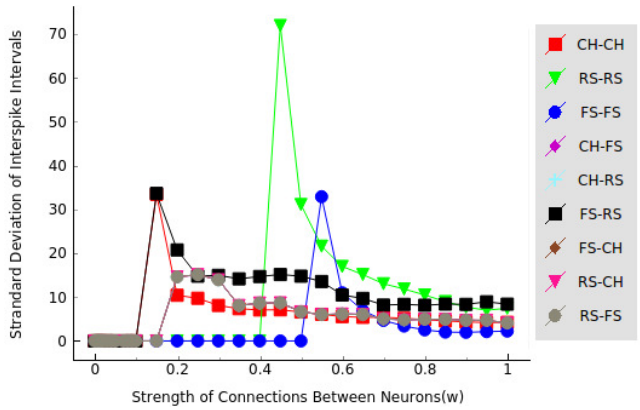

FIGURE 2.10: The y-axis shows the standard deviation σ_{Is} of Is. Each configuration shown is the average of 10 experiments. The inter-spike interval was measured in ms. When w is in the range of 0 0.1, the post-synaptic neuron do not spike and the ISI value is set to zero.

We now connect an external input to the post-synaptic neuron n to understand the aspect of the influence of external signals on the phase-locking process. In Figure 2.11 we show the time dependent plot of the two neurons superimposed as in figure 2.6. Now that both neurons are spiking, phase locking is reached sooner than before, the correlation dependence with w

grows faster and the onset differentiation between neuron types combinations is minimal (figure 2.15 (b)). In this case, the phase space of the system, shown in figure 2.12, suggests a very quick synchronization between the two neurons. Also, the system appears to be extremely sensitive to the connection parameter w, since even at $w = 0.01$ already a certain level of correlation is observable in the phase space, inset (a) of figure 2.12.

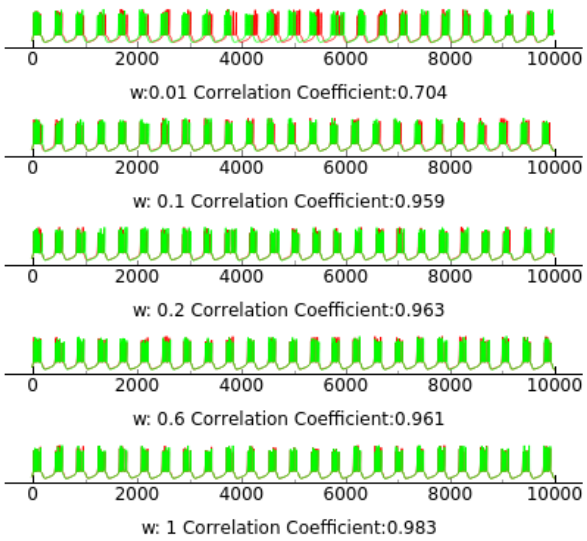

FIGURE 2.11: Two CH-Ch neurons are connected to an identical external current and reach high level synchronization level for $w = 1.0$.

This precise phase locking has been for example observed in couple of neurons by Stich and Verlade[70] using a similar coupling topology. The main difference of our tests with that study is that synaptic conductance was freely changing dynamically accordingly to predetermined rules, whereas in this research we control it systematically to elucidate its influence in the system in detail .

The figures 2.13 and 2.14 show the average inter-spike interval μ_{ISI} and the corresponding standard deviation σ_{ISI}. In the figures, both neuron n and neuron m had a stimulus of 8 mA. In this conditions the inter-spike interval of most of pairs do not change appreciably. However, an exception is the FS-RS system, where the properties of frequency acceleration and adaptation of these neurons come in to play [30, 48, 22].

Neurons belonging to the same class(CH, RS, FS) exhibit random differences in the four Izhikevich model parameters a, b, c and d to emulate natural heterogeneity and to avoid possible accumulation of systematic artifacts or errors due to repeated computation on identical systems. For the same

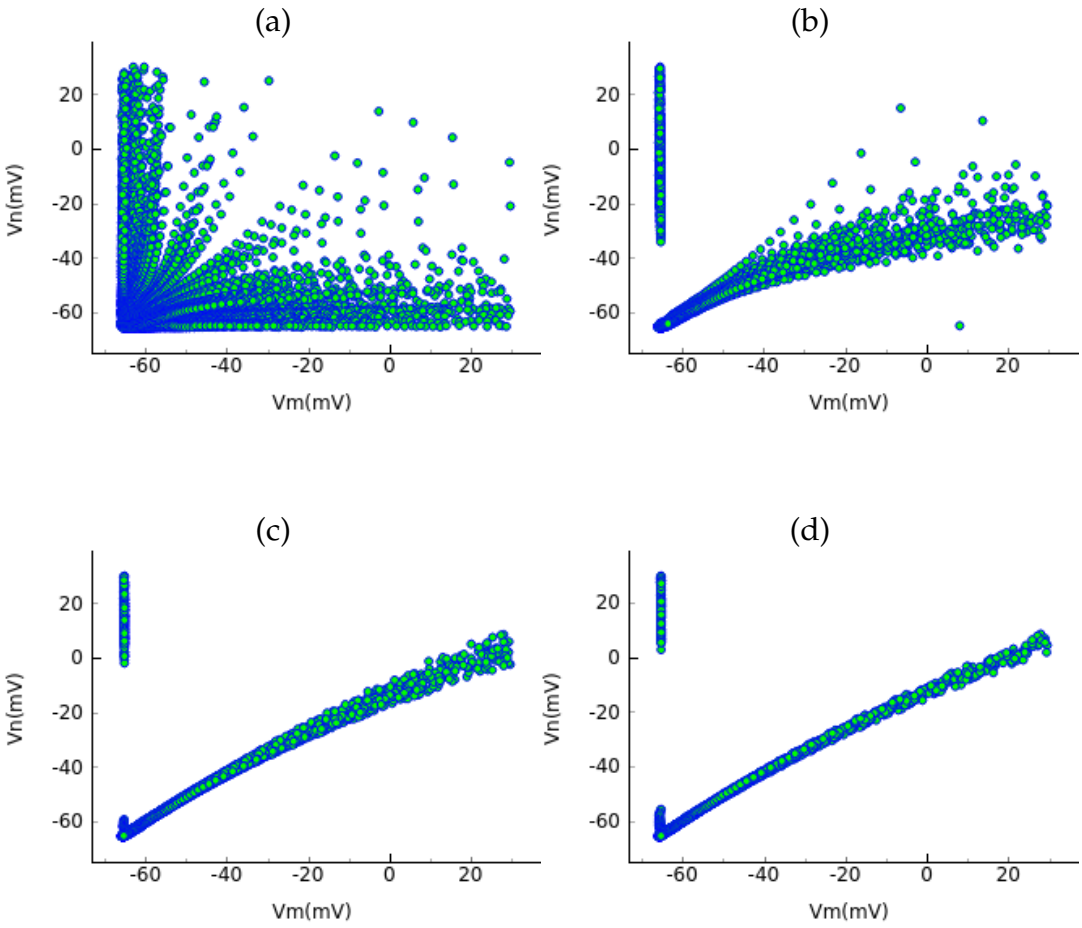

FIGURE 2.12: Phase space of the dynamics of the two neurons connected as in configuration B if m and n are both CH neurons. Vertical axis shows the action potential of neuron n and the horizontal axis the one of neuron n. In (a) the connection strength w is 0.01 increasing w to 0.1 in (b) correlation goes to 0.59 and then to 0.96 and 0.98 for $w = 0.6$ and $w = 1.0$ in (c) and (d) respectively. Compared with tests of figure 2.7, the synchronization reached higher levels and without discontinuity in w. This plot is made by averaging ten different tests.

reasons, simulations have been run ten times and their values were averaged, each dot in the plots of figure 2.15 (a) and (b) represents 10 different experiments run with different random seeds. In these plots, the connection strength w was varied from zero to 1.0 in steps of 0.05, except for the initial range 0 to 0.1 that is divided in more detailed 12 steps of about 0.008 for better representing initial threshold crossing transition.

As demonstrated in previous studies[26, 54], low and high frequencies inputs will influence the synchronization. Our results for the configuration

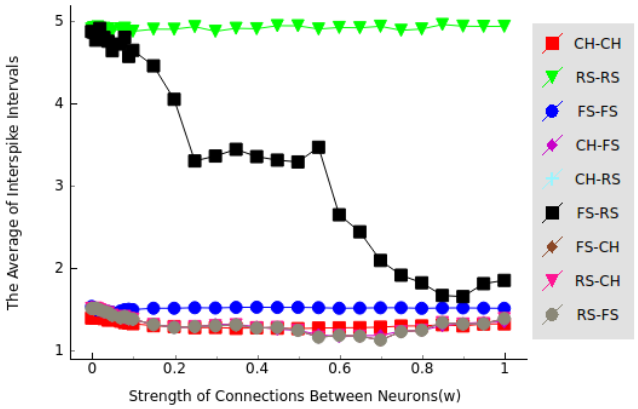

FIGURE 2.13: The y-axis shows the average of inter-spike interval μ_{ISI} of the post-synaptic neuron n. Each data shown is the average of 10 experiments. The inter-spike interval was measured in ms.

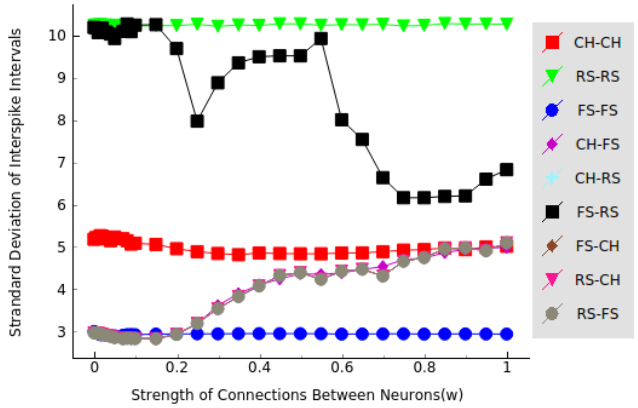

FIGURE 2.14: The y-axis shows the standard deviation of the inter-spike interval of the system σ_{ISI}. Each point shown represents the average of 10 experiments run with different random seeds. The inter-spike interval was measured in $msec$.

A (see figure 2.15 (a)), show that if the input spike train has high frequency components (when the pre-synaptic neuron is of type FS), the system synchronize and lock with difficulties compared with the other cases with pre-synaptic CH or RS. Noticeably, all curves related to a pre-synaptic FS neuron are grouped at higher connection strength w with threshold of about $w = 0.5$ instead of lower w for the other cases. Also notice that pre-synaptic RS neurons are found in adjacent position for intermediate w and finally pre-synaptic CH neurons instead appear to be the best *pace maker* locking sooner at lower connection strength of about $w = 0.1$. This is suggesting that the fast firing of multiple stimuli in the burst has better chances to find the appropriate time window to make the post-synaptic neuron internal state to resonate into a synchronized spike[2].

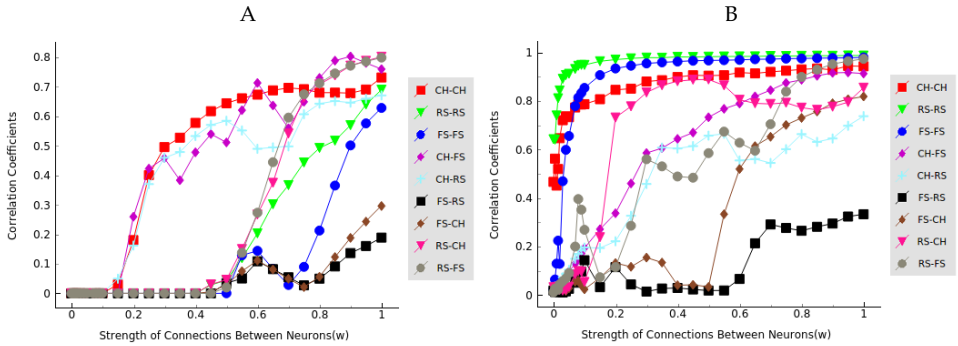

FIGURE 2.15: Configuration A (figure (a)): The behaviour of the correlation coefficient ρ in function of correlation strength w. In this plot only the pre-synaptic neuron m has an external continuous stimulus. Symbols like CH-RS represent the type of neuron acting on which type of neuron with the pre-synaptic one on the left and the post-synaptic on the right. Every dot in the plot represents the average of ten different test simulations. Each of these simulations is done over 100000 points and run with small random fluctuations on the neuron parameters to avoid artifacts. Configuration B (figure (b)): A plot of correlation coefficient against connection strength taken in similar condition as figure 2.15 (a) and figure 2.13. In this case, both of the neurons have an external continuous stimulus. These two plot show clear differentiation between type of neurons. Notably CH types appear to be the best to induce synchrony at low w, whereas FS-RS in all cases show lower level of correlation. Also, FS-RS configuration appear to behave uniquely also in the plots of figures 2.13 and 2.14, where ISI changed significantly with the variation of connection strength.

In configuration B, as shown in figure 2.15 (b), both of pre-synaptic and post-synaptic neurons are stimulated by a constant input $I = 8\ mA$. Here, differently from above, if the pre-synaptic and post-synaptic neurons are of the same kind, they synchronize rapidly at very low values of w. Similarly to configuration A, pre-synaptic FS class neurons have difficulties to lock the system and this results again in a higher threshold value. The threshold value of w for pre-synaptic CH class neurons and RS class neurons is about 0.2 but in the case of pre-synaptic FS class neurons, the threshold value moved to 0.5.

The FS-CH case is a noticeable because after an initial growth and plateau tendency at about $w = 0.4$ correlation drops again until a second rise at $w = 0.5$ and a similar behavior is observed also for the RS-FS couple. This suggests that the FS prominent feature of spike frequency adaptation, the

tendency of neurons to relax its inter-spike time so decreasing its instantaneous spiking frequency, hinder conspicuously the phase lock process in a strongly non linear fashion compared to other configurations [15, 30].

Chapter 3

Noise influence on spike activation in a Hindmarsh-Rose small-world neural network

3.1 Introduction

The control and flow of information in Brains is fundamental for the understanding of high-level processes like attention, visual perception and other complex functions[79, 63]. Despite enormous system complexity, it has been found that information can be sourced by single neurons even in major sensory pathways[58]. These distinct units can trigger chain of events that contribute to complex perception episodes or high level motor responses. This is known to happen for example with features detectors neurons[43] in lower animals, and similar phenomena are observed in mammal's neurons of higher hierarchical position in the visual system, those that respond to complex patterns and activate elaborate responses[50].

Despite the great volume of experimental facts that points toward noise as a contributing factor in signal transmission in brains[1, 29, 46] or generally in non-linear networks [46], we do not have yet a universally accepted theoretical framework to quantitatively evaluate the effects of noise to neurons operations and to the higher level network functions.

Here we want to contribute to this problem with a study in which we emulate a triggering event in the brain through a single active neuron that we call *initiator* x_o and, in controlled noise conditions, we study the flow of spike activity along the network to evaluate the role of noise amplitude on the signal propagation. In the first part of this study, we elucidate in a quantitative manner the role of noise and we found for the first time a linear relationship between the amplitude expressed in decibel and the delay interval between initiator x_o first spike and the network activation. Moreover, studying the

dependence with network size, we found that as the network grows in dimensions, the spiking activity starts earlier until the role of the initiator is completely suppressed beyond about $N = 100$ neurons. In the second part of the research, we characterize the network especially focusing on the spectral characteristics, going in details on its frequency dependence with noise and size. It is found that high levels of noise introduce chaos in the network and that, again, network size seems to replace the function of external noise for simulations with constant noise level and variable network sizes.

3.2 Models and methods

We used a Newman−Watts small world network to simulate the neural network. A realistic neural network is neither regular nor completely random[37] and this network has both deterministic and random properties[52]. Simulation of relatively small artificial networks can be a good metaphor for real brains as, for example, in 2003 Izhikevich demonstrated that a network of simulated spiking neurons exhibited collective waves and frequencies [34] in a range similar to the human brain.

To simulate the neurons we used the Hindmarsh−Rose model[7, 66] changing the intensity of noise and the network size to elucidate the role of spiking frequencies in function of various parameters. Even though precise arrangement of neural connections in real brains is not known, Small-World network models are widely used to simulate known statistical properties of Brain's neural connections, reproducing high clustering coefficient and low shortest path[53, 6, 85, 51]. The network random connection probability of the Small-World structure has been kept to $p = 0.4$ as a reasonable value with enough random connections to induce fast diffusion of spikes, but still small enough to represent real biological systems. This network structure and p values are considered reasonable on numerous literature studies, for example Basset[6] where regions of Human brain are found to have clustering coefficient as low as 0.14 equivalent to $p > 0.4$, or also Yan H.Z[87] and Ozer[56] for values of $0.1 < p < 0.6$ in small-world neural networks. To measure the global behavior of the network we monitored the integral of the total membrane potential. This is considered to be analogous to the electroencephalogram (EEG) in a real brain. By means of Fourier analysis, we found that this collective signal has distincts frequency peaks which are compatible with values observed in biological systems. This fact is not trivial since neuronal activities of a complex network are very difficult to predict analytically.

The Hindmarsh−Rose[27] system is characterized by three independent variables that represent the membrane potential and the two ion channel currents. A single neuron model is described by the following differential equation:

$$\begin{cases} \dot{x} = y - ax^3 + bx^2 - z + I \\ \dot{y} = c - dx^2 - y \\ \dot{z} = r[s(x - \chi) - z]. \end{cases} \tag{3.1}$$

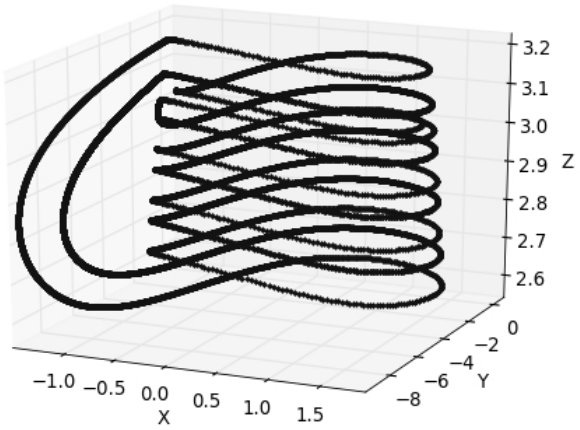

FIGURE 3.1: Simulation of a Hindmarsh−Rose model for a single neuron not affected by noise or connections. This shows the dynamical behaviour of the membrane potential. The variable *x(t)* represents the difference of voltage between extracellular and intracellular potentials. Spiking Variable *y(t)* instead describes the rate of change of the fast ion channels (sodium ion, potassium ion, etc.) and *z(t)* has similar meaning for the slow ion channels (calcium).

In this equation, x is time dependent and represents the membrane potential, whereas y and z are often called the spiking and bursting variables, respectively[18]. Those variables are all expressed in arbitrary units and do not have a direct translation in biologically realistic parameters[27].

In figure 3.1, it is shown a plot of the three variable phase cycle that induces the spike. The choice of the eight parameters in the model results in the kind of neuron simulated. Here we fixed them as $a = 3$, $b = 3$, $c = 1$, $d = 5$, $s = 4$, $r = 0.00$, $\chi = -1.6$ determined in order to produce neuronal bursting dynamics comparable to realistic neurons of "chattering" type. The *initiator* neuron x_o introduced above has a continuous input stimulus of $I = 3$ (a.u.) and starts at $t = 0$ with the initial values *x(0)*=0.3, *y(0)*=0.3, *z(0)*=3. Other authors[65] use similar values of input currents, ranging from about $I = 2$

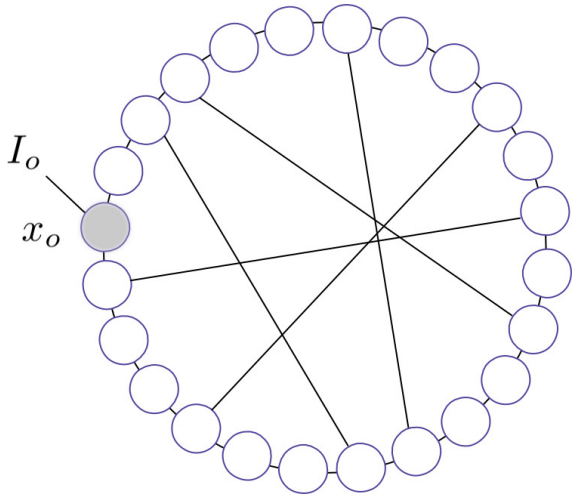

FIGURE 3.2: A sketch of the network structure. Each neuron is represented by a circle and simulated by the Hindmarsh−Rose model. The lines represent neural connections to neighbors neurons. The random connections that cross the circle are those due to the p parameter of the Small-World structure. The grayed neuron indicated by the symbol x_o a special *initiator* that has a constant external current input I_o and it is used to stimulate the whole network and to study the diffusion of spikes in the system in presence of noise. In our simulations the connections are changed randomly at every run, however the Small-World structural parameters are maintained constant. The cross connections parameter p is kept at $p = 0.4$ (for image clarity in this sketch p is lower). In some experiments the number of neurons is also varied.

to $I = 10$. Other neurons initial current values are set to zero. This neuron is called *initiator* because of its role of single source of information in the network. In other terms, the *initiator* x_o is the only neuron that provides stimulated spikes and those are thought as the single source of information in the network. That is, in absence of external noise, if other neurons are spiking it is because directly or indirectly they receive the information to do so from x_o. Our study investigates throughout the role of noise in this context. The entire network is connected as a Small-World system, without exception of x_o that receives input from the neighboring neurons accordingly to the network structure, see Figure 3.2 for a sketch of the configuration used.

The integration of the differential equation (3.1) is done with an Euler method, a time consuming but straightforward integration method. Time step is set to $\Delta t = 0.01$ ms [84] and has been verified to not introduce instabilities (slight increase of Δt does not provoke appreciable variation in the network response)

Figure 3.3 shows the Fourier transformation of the membrane signal of a

single neuron inserted in a $p = 0.4$ network. The network itself is intentionally chosen to be smaller ($N = 10$) and with the minimal noise level (signal to noise ratio $dB = 40$) in order to be an example of frequency signature of the neuron response. The neuron position is chosen at random far from the active x_o. Very interestingly, we can observe the emergence of peaks at 10 Hz, these frequencies in the averages membrane potential can be though as an analogous of α waves in real brains. This shows biological plausibility in simulations as already established for example by Izhikevich. [35, 57].

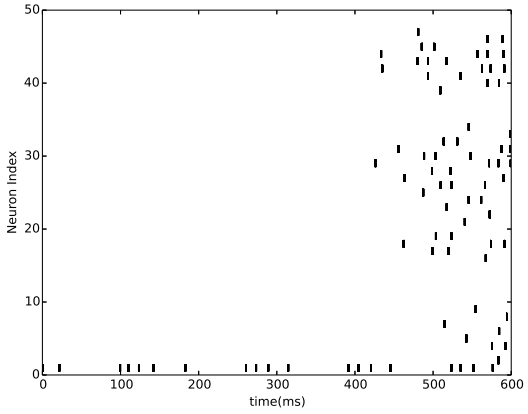

FIGURE 3.3: The Fourier transformation of the membrane signal of a single neuron inserted in a $p = 0.4$ network of $N = 10$ and with signal to noise ratio $dB = 40$. This is an example of frequency signature of a single neuronal response. The inset shows the actual spike plot where the Fourier transformation was calculated from, the horizontal axis represents 1000 msec of time. The bar at $x = 0.8$ indicates the threshold used to separate the baseline activity from the action potential. The neuron is chosen at random and it is not connected to the initiator neuron x_o.

To generate the network, firstly, we create a regular network with a ring over n vertices. Each vertex stands for a neuron. Then, every vertex in the ring is connected with its nearest neighbors at both sides. In all our tests, $k = 1$, this means that each neuron is connected with two neighbors, one on its left and the other on its right. We say that the network is of dimension $k = 1$ (if $k = 2$ each neuron has four neighbors, two on the left and two on the right). Starting from this regular network structure, we create random shortcuts by adding connections pointing to other neurons chosen at random with probability p ($p = 0.4$ in our case). Each vertex v_i ($i \in \{1, 2, 3...N\}$) can be connected with any other with probability p. For vertices v_i and v_j, a uniform distribution random number in the range zero to one is generated

and compared with p. If the number is lower than p the connection between v_i and v_j is created, otherwise not. A similar test is done to the adjacent neuron until all neurons are examined. Neurons have no connections with themselves and two neurons can be coupled by a unique segment, a single neuron can receive more than one connections from different neurons[77].

A good representation of biologically plausible noise is controversial, however since the central limit theorem guarantees that a good number or arbitrary distributes sources converge to a Gaussian signal, we opted for this type of noise[5, 81, 14]. The intensity is modulated using different values of signal-to-noise ratio (SNR) defined in decibel as $dB = 10\log_{10}(\frac{A_s}{A_n})^2$. Where A_s is the amplitude of the signal and A_n that of the noise. We use this definition because is standard and logarithmic, however we have to empathize that bigger values of dB mean a less noisy network.

The random variable is generated with this formula :

$$\phi(X, \mu, \sigma) = \frac{1}{\sigma\sqrt{2\pi}} e^{(\frac{-(X-\mu)^2}{2\sigma^2})}. \tag{3.2}$$

Here X is a flat pseudo-random value generated internally by the numerical library *numpy*[36, 75], μ is the mean value around which the Gaussian is centered and σ is the corresponding standard deviation. In our experiment, μ was fixed as 0 and σ as 1[82][19]. We use

$$\begin{aligned} S &= \frac{1}{N}\Sigma_i x_i, \\ \eta &= \sqrt{\frac{S}{10^{dB/10}}}, \\ \varepsilon &= \eta\phi(X, \mu, \sigma). \end{aligned} \tag{3.3}$$

N is the total number of neurons, x_i the membrane potential of neuron i, η the noise amplitude and ε the final Gaussian noise random variable. It results to be distributed along a Gaussian curve, with intensity proportional to η that contains the decibel parameter that is varied in the tests[40]. The intensity of noise is calculated at each time loop, so several neurons receive the same noise intensity for the same time step. This is an approximation of a realistic network where noise do not have spatial specificity.

The differential equation that describes the time evolution of a single neuron x_i in the system is:

$$\begin{cases} \dot{x}_i = y_i - ax_i^3 + bx_i^2 - z_i + \varepsilon_i + g_i \sum_{j=1}^{N} a_{ij}(x_i - x_j) + I_o \\ \dot{y}_i = c - dx_i^2 - y_i \\ \dot{z}_i = r[s(x_i - \chi) - z_i]. \end{cases} \tag{3.4}$$

This formula is equivalent to eq. 3.1 but extended for a system of N neurons, variables and parameter have the same meaning explained previously. The index i represent each of the N neurons in the network. The parameter ε_i is the Gaussian noise of neuron i, updated at each time loop. To compute the input current that each neuron receives, we calculate $g_i \Sigma_{j=1}^{N} a_{ij}(x_i - x_j)$. The sum is mediated by an adjacency matrix a_{ij} that stores the connection between the vertices. In it, a_{ij} is 1 if there is a connection between the neuron i and j, otherwise it is 0. x_i and x_j are the membrane potential of neuron i and j. g_i is the coupling strength[76, 4] that is normalized to the number of connections of neuron i. In this way:

$$g_i = \frac{1}{\sum_{j=1}^{N} a_{ij}}. \tag{3.5}$$

In this formula, N is the number of neurons in the network. If we do not impose this normalization, the network will have an unbalanced influence of signals coming from the neighbors neurons depending on connections number[83, 69].

As stated above, in our simulation a neuron x_o receives a specific continuous current stimulus I_o that is set to a value of 3 (a.u.) in all our tests. So, in the first equation of system (3.4) if $x_i \equiv x_o$, $I_o = 3$, in all other cases $I_o = 0$.

3.3 Results

We verified that without the contribution of the special initiator neuron x_o, the network exhibits no spiking activity and membrane signal settle to a baseline value.

On the other hand, if neuron x_o receives a constant input I_o it becomes active and drives its connected neighbors to spike, and those will induce spiking on their neighbors. The information will propagate until the whole network will be spiking in a random but stable manner.

In the following tests, corresponding to figures from 3.4 to 3.7, a network of N =48 neurons was used with connections as in table 3.1, i and j are the index of neurons. Value 1 in each grid indicates neuron i is wired with

neuron j ($a_{ij} = 1$). Empty grid means there is no connection between neuron i and neuron j ($a_{ij} = 0$).

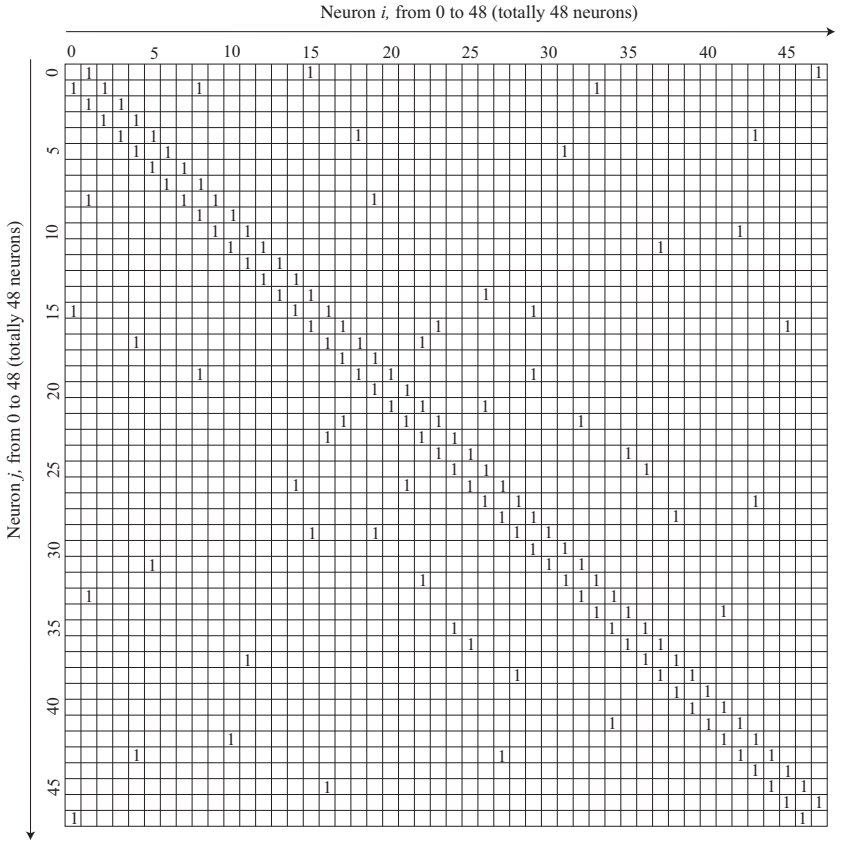

TABLE 3.1: An example of network connections. Values of a_{ij} represent the connection strength within the 48 neurons small-world network. Connection strength can be only of value 1 (connected) or zero (not-connected). Zero values are not shown for clarity).

Noiseless response of such a system is shown in the spike map of figure (3.4). This map is generated using an arbitrary threshold to separate basal random signal from the spikes. After few tests to evaluate the membrane potential range, the threshold was chosen as *x=0.8*, see inset of figure (3.3). When the membrane potential exceeds this value, we assume that the neuron is firing[59] and plot the mark that is shown in figure (3.4) and the following spike maps. To evaluate the behavior of the network as a whole, we integrate the membrane potential for the entire population of neurons. We use this equation to calculate the parameter $E(t)$:

$$E(t) = \frac{\sum_{i=1}^{N} x_i(t)}{N}. \tag{3.6}$$

In figure 3.5 we show the output of the network measured as the average membrane potential calculated with eq. (3.6) for a network of 48 neuros,

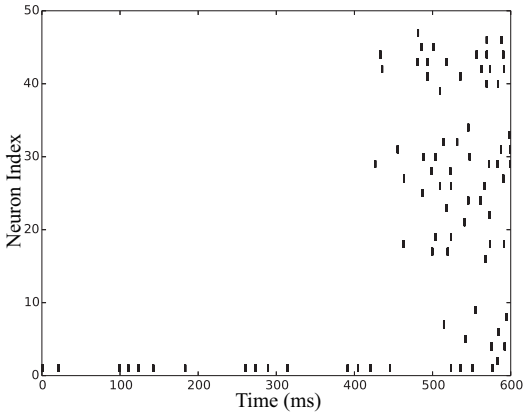

FIGURE 3.4: The spike map of a noiseless small-world network of 48 Hindemarsh−Rose neurons, a sketch of it is in figure 3.2. The neuron indicated as number 0 is a special one that is connected to an external signal of $I = 3$ (a.u.) constant input. It functions as an *initiator* and after a delay of time, provokes the spiking of the whole network. The same experiment reproduced with identical parameters but with no external input ($I = 0$), produce no spiking everywhere in the network (blank result not shown).

$p = 0.4$ and $k = 1$. Clearly as the noise increases, the initial transitional behavior get shorter and shorter. This suggests two things, noise influences the average baseline of neuronal response and it affects also the spike rate of the neuronal system.

Figure 3.6 shows the raster plot for a neuron network with 48 neurons, $k = 1$ and $p = 0.4$ as before, for different noise levels. Again, the initiator neuron x_o is spiking since the beginning, whereas the rest of the network is quiescent and responds with a variable delay that depends on noise level.

The signal to noise ratio influences strongly the initiation of secondary spiking along the network. Calling S_s the time interval by which secondary spikes are activated, we can interpolate our results with a liner model

$$S_s = \delta\varepsilon + \alpha.$$

where $\delta = 14$ msec per decibel, ε is the noise level in dB and α is an offset, the linear regression coefficient is better than 0.9. The influence of the initiator x_0 is negligible and the linear dependence is clear. See figure (3.7) for graphical representation of this with a test with several level of noises. This formula cannot have a general meaning because it is bind to this specific network, however it shows a quantitative relation to modulate transfer of information

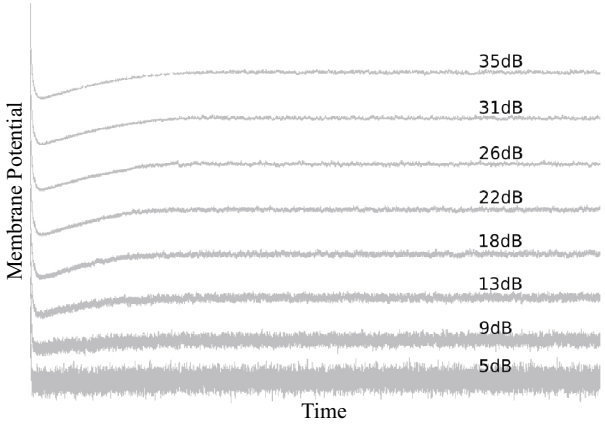

FIGURE 3.5: The behaviour of the neuron population membrane potential in function of noise level. Noise seems to help the diffusion of spikes along the network. Horizontal axis spans over 1000 ms of simulation calculated in 100,000 steps of 0.01 msec each. The vertical axis is the voltage in arbitrary units. Each simulation is taken on a network of $N = 48$ neurons and averaged on 8 different experiments done with same parameters but different random generator seeds. As the signal to noise ratio grows (less external noise) the initial transition time gets longer indicating a worse diffusion of information across the network.

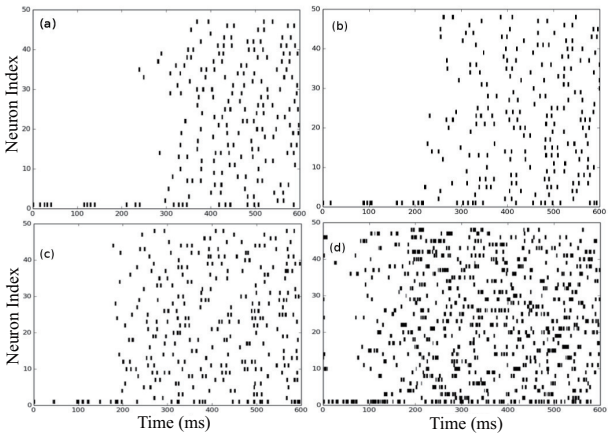

FIGURE 3.6: The spike maps of a network with $N = 48$ neurons in different noise conditions. Signal to noise ratio in each plot is (a) $dB = 35$, (b) $dB = 31$, (c) $dB = 26$ and (d) $dB = 18$. The signal to noise ratio influences strongly the initiation of regular spiking along the network. On the vertical axis we have the neuron number, neuron indexed as zero is the special *initiator* neuron x_o. Notice that a better signal to noise ratio means less external noise. Intermediate dB values were calculated but not shown.

with noise intensity in this case.

A network with identical parameters as above was tested in similar way

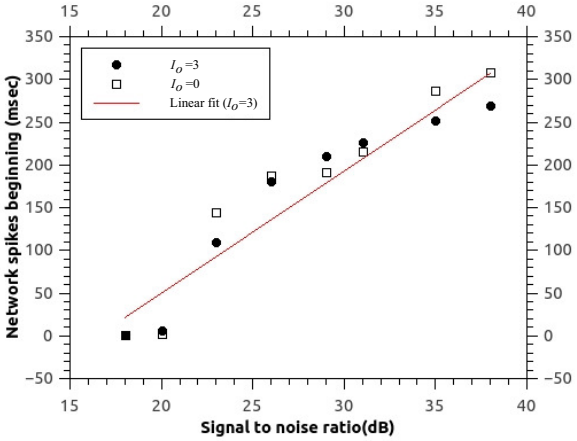

FIGURE 3.7: The comparative plot of the delay by which the spiking activity starts in a network with and without an active initiator x_o. Round dots represent the delay with an active ($I = 3$) initiator and the square an inactive one. The influence of x_o is negligible and linear dependence is clear. The red line represents a linear interpolation of $r > 0.9$ and inclination $\delta = 14$ msec per dB.

but changing the size of the network instead of noise (noise level was kept constant at 20 dB). As shown in figure 3.8 for small network sizes the initiator neuron x_o makes the spread of spikes quicker, but it does not seem to influence strongly the transitional delay period after the network grows more than about $N = 100$ neurons.

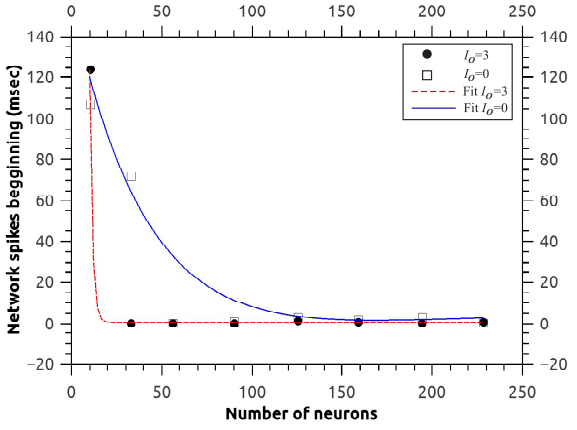

FIGURE 3.8: The comparative plot between networks with and without an active spike initiator x_o, in the same fashion as in figure 3.7, but when the network size is changed. For small network sizes of less than about $N = 100$ neurons the initiator makes a difference and induce quicker propagation of spike activity. The noise level is kept to 20 dB in all the tests.

To analyze the influence of noise to the collective frequencies of the network, we studied the Fourier spectrum of the variable E in (3.6). The Fourier spectrum peaks, if present, are very important for recognizing rhythms and regularities in the entire network that mimic the biological phenomena of slow and fast waves in real brains.

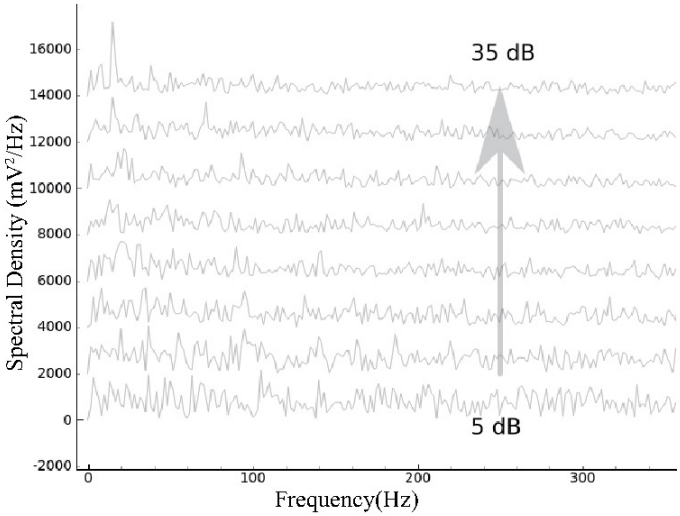

FIGURE 3.9: A plot of the fast Fourier transformation of the membrane potential averaged over the whole network. The curves represent the frequency spectrum of it averaged over the whole network. Each line represents a simulation with different level of noises. The horizontal axis is in Hz and the vertical in arbitrary units. The latter has a relative meaning since plots are shifted vertically for clarity. These show how the network characteristic frequencies are influenced by different noise levels. The simulations are produced with a total of $N = 48$ neurons. The small world network is characterized by a connection probability $p = 0.4$ and dimension $k = 1$ and a spiking *initiator* neuron x_o with input $I = 3$ (a.u.). The plot considers only the frequencies at regime. That is, the simulation is for 1000 msec, the first 300 msec of data are not considered, in order to avoid low frequencies due to the initial baseline variations. Each plot is the average of 8 identical simulations executed with different random number seeds. The influence of an active ($I = 3$) or passive ($I = 0$) neuron x_o is null since we obtain equivalent results in both cases.

The Fourier transformation presents evident peaks at strong signal to noise ratio (top curve, $dB = 35$), whereas the more prominent peaks at α and β seem to decay with increasing noise[35], see figure 3.9. The Fourier transform data are calculated over a simulation period of 1000 msec, cutting off the first 300 msec to avoid including slow frequencies due to the initial transitional phase discussed above. Interestingly the prominent β peak seems

to shift to the right with noise intensity, a very weak effect that is, however, difficult to prove with mathematical means. We studied the total network power average among 5 different frequency bands, θ, α, β, γ_1 and γ_2. We calculate the Fourier spectrum of a 1000 millisecond simulation as above, then we sum up the power of those five frequency bands with this formula

$$\begin{aligned}
\theta &= \frac{1}{N_\theta}\Sigma_{f=4}^{7}\Psi(f)df, \\
\alpha &= \frac{1}{N_\alpha}\Sigma_{f=7}^{14}\Psi(f)df, \\
\beta &= \frac{1}{N_\beta}\Sigma_{f=14}^{30}\Psi(f)df, \\
\gamma_1 &= \frac{1}{N_{\gamma_1}}\Sigma_{f=30}^{40}\Psi(f)df, \\
\gamma_2 &= \frac{1}{N_{\gamma_2}}\Sigma_{f=50}^{70}\Psi(f)df.
\end{aligned} \tag{3.7}$$

Here Ψ represents the vector that contains the module of the fast Fourier transformation array. The elements corresponding to frequencies within the band are added up (θ from 4 to 7 Hz, α 7 to 14 Hz, β 14 to 30 Hz, γ_1 30 to 40 Hz and γ_2 50 to 70 Hz). Each band has different number of elements, so the value is normalized to the various N_θ, N_α etc., depending on how many elements each band has. Then we plot the result against the noise, figure 3.10.

In this plot we see that all prominent peaks decrease with noise intensity. This happens because low level of noise produces the transitional phenomena shown in figure 3.6 and 3.5, during which few neurons are spiking, then the network goes to a regime with lower and more distributed frequency peaks. To verify that these patterns are indeed due to the initial transitional phenomena and not by an intrinsic character of the network, we cut off the first 300 msec of simulation and we instead observe a more intricate behaviour of the bands power, shown in figure 3.11.

Since each symbol represents a different noise level, the fact that the plots intersect each other indicates that noise produce a non-linear effect frequency bands amplitudes in this case. We investigate the network changing the network size as a paradigm of biological internal noise. The analysis is conducted with other important neuron properties and characteristics kept constant to allow comparison and discussion. Small world dimension $k = 1$, probability $p = 0.4$ and every simulation is repeated 8 times with different random seeds, then averaged as in the previous tests.

As shown in figure 3.12, each spectrum shows distinct peaks in the α and

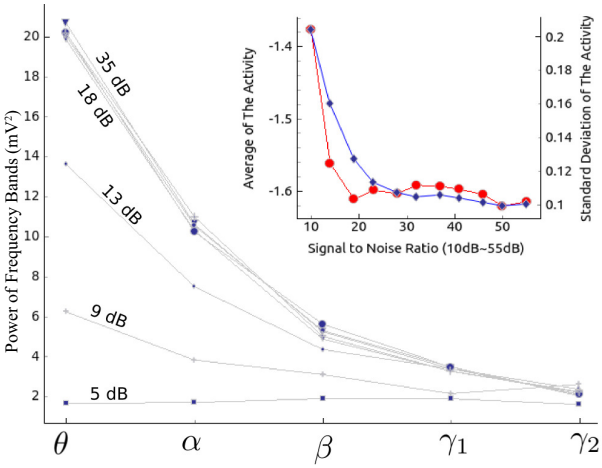

FIGURE 3.10: The power of five frequency bands for a network of $N = 48$ neurons. The level of noise is represented by each symbol according to this scheme: square, $dB = 5$, plus, $dB = 9$, diamond, $dB = 13$, triangle, $dB = 18$, triangle (bigger), $dB = 22$, circle, $dB = 26$, circle (bigger), $dB = 31$, plus (bigger), $dB = 35$. The peaks magnitude seems to keep the same relative order with noise, this effect is caused by the predominance of the initial transition to regime over the noise influence. The inset shows the average and standard deviation of $E(t)$ in function of noise for the same network. The average potential drops regularly because of the initial transitional period that drives potentials to more negative values. Noise reduces this initial transition, so the curve appears less negative at low dB values. Refer also to figure 3.5. For reason of clarity not all the decibel labels are indicated.

θ range. Interestingly, this behavior is maintained also for bigger networks. At present conditions, our system is limiting the simulations to these network sizes, but it would be interesting to increase even more the number of neurons to see if the diminished lower frequencies peaks phenomenon observed with external noise increase would be repeated with networks of much higher sizes.

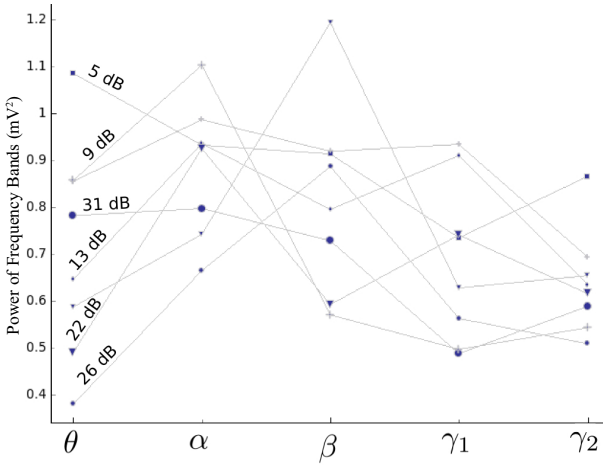

FIGURE 3.11: The power of five frequency bands for a network of $N = 48$ neurons at different noise levels as in figure 3.10. Noticeably, the first 300 msec of simulation where cut off to emphasize the network frequencies at regime. The various plots cross each other, with no systematic trends. This is indicating that the noise is influencing the spectrum relative intensities and seems to shift peaks position (see figure 3.9). For reason of clarity not all the dB labels are shown. The initiator x_o has negligible influence on these plots, see figure 3.7.

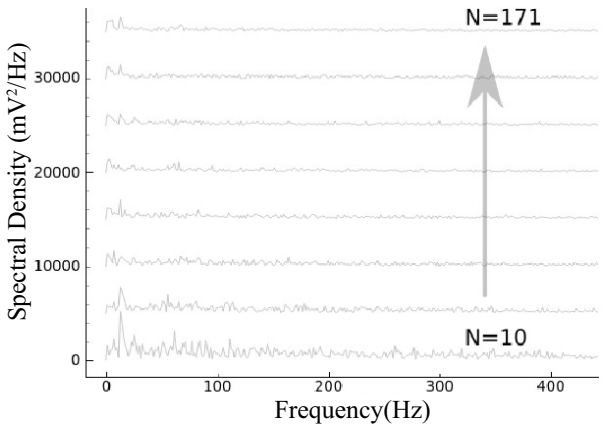

FIGURE 3.12: The Fourier transformation of the membrane signal in networks of different sizes and constant 20 dB noise level. Each line is shifted vertically for clarity, in the same fashion as figure (3.9). From top to bottom, the number of neurons is decreasing (top 171, bottom 10 with steps of 23 neurons). The simulation is run for 1000 msec, first 300 msec of data are not considered to avoid low frequencies due to the initial baseline variations. Frequencies peaks emerge in all conditions, but less prominent for networks of bigger sizes. Each plot is the average of 8 identical simulations executed with different random number seeds.

Chapter 4

Discussion and Conclusion

In this research work I succeeded to clarify two important things, the role of synaptic connectivity in a minimal two-neuron system and the way information propagate in a model neural network.
I chapter 1, we have focused on the synchronization of a pair of neurons and studied the spiking correlation using a coefficient ρ. We have shown for the first time that correlation is highly non-linear in w with the presence of distinct threshold points for all neurons classes studied. Synchronization in simplified system of two neurons has been analyzed with real isolated coupled neurons by Elson [21] and with analog electronic neurons by Pinto[60]. Innovative numerical simulations has been performed by Wei[78] and Stich[70], however no systematic study on the neurons synchronization against coupling coefficient was elucidated in previous studies. We found that when the threshold point is crossed two neurons reach a state of synchronous spiking that is characterized by a bifurcated and asymmetric phase diagram (figure 2.7(d)). This behaviour is similar to what has been found in the work of Pinto et. al that studied an electric analog neurons model[60]. Non linear behaviour is evident in the inter-spike interval plots for all class of neurons tested and clear differentiation between neuron types has been found and reported in figures 2.9 and 2.10. Interspike activity begins at transition points that make the threshold crossing phenomena more evident. In addition to all previous literature knowledge, we have shown that neuron class radically changes the response of the system to connection strength. Inter-spike interval is kept almost invariable for two neurons stimulated by a constant input for any connection strength, however evident inter-spike drift is observed for FS-RS pairs (figure 2.13). The dependence on neuron types is even more evident in the inter-spike distribution width (represented by the standard deviation in plot of figure 2.14). Prominent threshold behavior is observed and shown in figure 2.15 (a) systematically for each neuron type pair combination. Striking differences in response and threshold values are observed and

reported, moreover, if the second neuron has his own external constant stimulus, again impressive differences in response, threshold and inclination of correlation curve are reported (figure 2.15 (b)). These quantitative observation and original behavioral features are the elemental foundation that may pave the way for the development of new brain theoretical models of small or larger networks.

The fact that discontinuity is found in the connection strength vs correlation plot is not surprising, since neural connections are known to hold a strong threshold dependent relation to input. In fact, simpler artificial neural networks are generally represented with sigmoidal-like curves in input. However, we found essentially two novel information in our study. The first is that this threshold is variable, and the variability depends strongly with the type of neurons that we are using. As visible in our data (figure **??**) chattering neurons are driving the post-synaptic neurons to correlation at an earlier value of connection strength than any other neuron. It is very important to notice that the threshold at which correlation between the two neuron rises, is virtually the same for the three type of post-synaptic neurons. The configuration CH-RS, CH-FS and CH-CH shows the same threshold value of about $w_0 = 0.2$, also shape of the curves is very similar for the three configurations and a plateau of $\rho \approx 70\%$ is reached for all of them. This striking similarity for three different neurons is striking and suggests that the level of correlation depends strongly on the pre-synaptic neuron type. Also, our results indicates that the brief bursting activity of chattering neurons is able to stimulate the dynamics of post-synaptics systems with the same strength even if the neural characteristics differs.

The fact that we have a real measurable threshold value (w_0) is useful to dimension, test and realize actual artificial system knowing in advance connection strength level of importance in a dynamical system. For example, in the case that the pre-synaptic neuron is of CH type, our work give neural systems designers the *a-priory* knowledge that connection strength less than 20% are not influential to the dynamics, as well as 50% or higher ws are not important since plateau is already reached. In the case of chattering neuronal system, the range of $0.2 < w < 0.5$ all what counts.

Same discussion can be deduced for the other neuronal configurations we studied FS-CH, FS-RS, FS-FS and RS-CH, RS-CH and RS-RS. Very interestingly, when the pre-synaptic neuron is of FS type, whatever is the post-synaptic, we notice a threshold at about $w = 40\%$ and a sort of secondary resonance peak at almost exactly $w = 50\%$. This peak is reproduced only in

the case of pre-synaptic of FS type, but not in the case of RS type, even if the threshold value corresponds. This again support the general conclusion that when a pre-synaptic neuron is driving a not-stimulated post-synaptic one, the pre-synaptic characteristics win on the pos-synaptic neuron. This fact is very important for the design of neuronal systems. In the right panel of figure 2.15 we show the situation in which the two connected neurons have their own independent stimulation. Also in this case we have have found very specific behavior that have meaning in a general neuronal system. The legend of the figure shows, the three systems where the neurons are identical (CH-CH, RS-RS and FS-FS) show immediate sensitivity to the connection strength w, without a visible threshold-like behaviour. Moreover, they lock quickly to high values of $\rho > 80\%$ reaching a plateau at $w < 0.2$. Noticeably the plateau is reached earlier than the initial threshold in the other connection model.

In chapter 2, We analyzed the collective behaviour of a H-R small world network of dimension $k = 1$ and random connection probability $p = 0.4$. The influence of noise is studied, especially concentrating on the effects it has on the propagation of information along the network by studying the membrane average frequencies and spike activity diffusion due to an active neuron that initiate the spiking. To isolate other effects the network is in ideal conditions, identical neurons, no plasticity and no delay time are considered. The network have a single active neuron x_o connected to an external stimulus of $I_o = 3$ mA. This neuron is spiking constantly and in absence of noise it induces the rest of the network to spike after an initial transitional time. Most interestingly, it seems that noise favors the initiation of secondary spikes (the spikes that follow those of x_o), and this spike activity becomes spontaneous and independent from x_o. We found a linear relationship between secondary spikes initiation time and signal to noise ratio in decibels, with an inclination constant of about $\delta = 14$ millisecond per decibels. This phenomenon is instead found to be much weaker or not existent if we increase network size. However, for networks of sizes of $N = 100$ neurons or less, the initiator x_o still makes a difference, favoring the quicker spread of spike activity on the network. This suggests that locally active neurons play a role in the spread of information in confined domains outside which the effect decays with distance. For the sake of simplicity and to avoid complexity this result has a limited meaning bind to the specific Hindmarsh$-$Rose network studied here, but we have intention to verify if this function of noise

is a general phenomenon in spiking networks or remains limited the conditions and network connection structure used. The importance of noise in neural networks is known, and what we observed reminds phenomena of stochastic resonance in biological systems[1, 67, 73, 45, 47]. The influence of noise on frequency have been investigated by Fourier analysis. We have shown that once the transitional delay is past, noise displaces main frequencies peaks, provoking a slow transition to chaos. Studying the most prominent frequency bands (θ, α, β and γ) we confirmed that noise quenches those biologically significant peaks in the network. Still, at regime, a less keen transition to chaos is observed, frequency peaks do reduce and tend to disappear, but in a slower and more complex trend that seems to conserve some activity in the $theta$ and $alpha$ band (cfr. figure 3.9 and figure 3.11). In real brains, the noise is generated internally, so we scaled up the network and used the network size as a paradigm of the external noise. We found two trends, a reduction in peaks amplitude and better sharpness and definition of Fourier peaks, but not an evident degeneration to chaos observed increasing external noise. This trend must be presumably confirmed with much higher network sizes, and we have intention to set up the appropriate computational tools to do that in the near future.
This two studies was related with two points. The first one we used the gap junction as the coupling way. The results showed the dynamics both in coupled neuron system and neural network with gap junction connections. The second one is in the two studies, we both analyzed coupled bursting neurons. Both gap junction and bursting neurons have important roles for information processing within brain. Recently, since the development of supercomputer, we can simulate huge networks, but we still don't have enough theories and basic methods to analysis the dynamics in complex networks.

Our study gives a basic theory and dynamics analysis method for simple neural systems. In the future, we would like to contribute to two different projects.

1. Improving the coupling neuron system what we introduced in Chapter 2 with Spike-timing dependent plasticity rules. We will focus on the influence of the time delay and the initial connection strength on the phases of spike trains. 2. Instead of small world networks, we will use grid networks and cube networks to construct our neural network system. In this system we will adjust the frequency of external stimulus, and we will observe more details about how the noise influence the information process in our brain.

In the past years, more and more people realized the importance of brain

research. Many countries started brain research projects. Even today, many artificial intelligence progress and deep learning applications show brain-like ability in many areas, but they are still not realistic intelligent systems. On the other hand, the study of brain's diseases and other medical related topics make a lot of social pressure. In brain research, computational neuron science has a very important role. This is because the process of neural information has a complex spatial-temporal structure. Using mathematical methods and simulations, we can focus on the significance of the activity of basic neural systems. For example we can study individual neurons or coupled neurons. Once those functions will be elucidated, we can analyze the average activity in neural networks with huge size or very complex structures with a better understanding of their functions and better control.

In conclusion using anatomy, EEG or other technologies, researchers have gathered huge of data when the brain perform particular tasks. Computational research like we did in our thesis, help the scientific community to create better brain models and using them to emulate particular behavior or activity that are observed in biological systems. Our study is contributing to the understanding on how real brains work and then figure out improved theories of our brain.

Bibliography

[1] Sygal Amitay et al. “Human Decision Making Based on Variations in Internal Noise: An EEG Study”. In: *PloS one* 8.7 (2013), e68928.

[2] Craig A Atencio and Christoph E Schreiner. “Spectrotemporal processing differences between auditory cortical fast-spiking and regular-spiking neurons”. In: *The Journal of Neuroscience* 28.15 (2008), pp. 3897–3910.

[3] Wyeth Bair, Ehud Zohary, and William T Newsome. “Correlated firing in macaque visual area MT: time scales and relationship to behavior”. In: *The journal of Neuroscience* 21.5 (2001), pp. 1676–1697.

[4] Stefan Balev, Nathalie Corson, et al. “Coupled HR Neurons: On the Influence of the Coupling Strength on the Neuron Dynamics”. In: *Proceedings of European Conference on Complex Systems 2012* (2012).

[5] JP Baltanas and JM Casado. “Noise-induced resonances in the Hindmarsh-Rose neuronal model”. In: *Physical review E* 65.4 (2002), p. 041915.

[6] Danielle Smith Bassett and ED Bullmore. “Small-world brain networks”. In: *The neuroscientist* 12.6 (2006), pp. 512–523.

[7] T Belykh et al. “Synchronization and graph topology”. In: *International Journal of bifurcation and chaos* 15.11 (2005), 3423–3433. ISSN: 0218-1274.

[8] Michael VL Bennett and R Suzanne Zukin. “Electrical coupling and neuronal synchronization in the mammalian brain”. In: *Neuron* 41.4 (2004), pp. 495–511.

[9] Guo-qiang Bi and Mu-ming Poo. “Synaptic modifications in cultured hippocampal neurons: dependence on spike timing, synaptic strength, and postsynaptic cell type”. In: *The Journal of neuroscience* 18.24 (1998), pp. 10464–10472.

[10] S. Boccaletti et al. “The synchronization of chaotic systems”. In: *Physics Reports* 366.1–2 (2002), pp. 1 –101. ISSN: 0370-1573.

[11] Dean V. Buonomano and Wolfgang Maass. "State-dependent computations: spatiotemporal processing in cortical networks". In: *NATURE REVIEWS NEUROSCIENCE* 10.2 (2009), 113–125. ISSN: 1471-0048. DOI: {10.1038/nrn2558}.

[12] Erik Cambria and Bebo White. "Jumping NLP curves: A review of natural language processing research". In: *IEEE Computational Intelligence Magazine* 9.2 (2014), pp. 48–57.

[13] Soni Chaturvedi, Neha R Sondhiya, et al. "Izhikevich Model Based Pattern Classifier for Hand Written Character Recognition–A Review Analysis". In: *Electronic Systems, Signal Processing and Computing Technologies (ICESC), 2014 International Conference on*. IEEE. 2014, pp. 346–349.

[14] Wang Chun-Ni et al. "Instability and death of spiral wave in a two-dimensional array of Hindmarsh–Rose neurons". In: *Communications in Theoretical Physics* 53.2 (2010), p. 382.

[15] Barry W Connors and Michael J Gutnick. "Intrinsic firing patterns of diverse neocortical neurons". In: *Trends in neurosciences* 13.3 (1990), pp. 99–104.

[16] Gabriela Czanner et al. "Measuring the signal-to-noise ratio of a neuron". In: *Proceedings of the National Academy of Sciences* 112.23 (2015), pp. 7141–7146.

[17] Jaime De La Rocha et al. "Correlation between neural spike trains increases with firing rate". In: *Nature* 448.7155 (2007), pp. 802–806.

[18] Daniel Terence DeBolt. "Application of the Hindmarsh-Rose neural model in electronic circuits". In: *Electrical and Computer Engineering Masters Theses* 56 (2013), pp. 8–13.

[19] Alain Destexhe and Michelle Rudolph-Lilith. *Neuronal noise*. Vol. 8. Springer Science & Business Media, 2012, pp. 405–409.

[20] Donald H Edwards, Shih-Rung Yeh, and Franklin B Krasne. "Neuronal coincidence detection by voltage-sensitive electrical synapses". In: *Proceedings of the National Academy of Sciences* 95.12 (1998), pp. 7145–7150.

[21] RC Elson et al. "Synchronous behavior of two coupled biological neurons". In: *Physical Review Letters* 81.25 (1998), pp. 5692–5695.

[22] Bard Ermentrout, Matthew Pascal, and Boris Gutkin. "The effects of spike frequency adaptation and negative feedback on the synchronization of neural oscillators". In: *Neural Computation* 13.6 (2001), pp. 1285–1310.

[23] Nathan W Gouwens et al. "Synchronization of firing in cortical fast-spiking interneurons at gamma frequencies: a phase-resetting analysis". In: *PLoS computational biology* 6.9 (2010), e1000951.

[24] Charles M Gray and David A McCormick. "Chattering cells: superficial pyramidal neurons contributing to the generation of synchronous oscillations in the visual cortex". In: *Science* 274.5284 (1996), pp. 109–113.

[25] Constance Hammond, Hagai Bergman, and Peter Brown. "Pathological synchronization in Parkinson's disease: networks, models and treatments". In: *Trends in neurosciences* 30.7 (2007), pp. 357–364.

[26] Andrea Hasenstaub et al. "Inhibitory postsynaptic potentials carry synchronized frequency information in active cortical networks". In: *Neuron* 47.3 (2005), pp. 423–435.

[27] JL Hindmarsh and RM Rose. "A model of neuronal bursting using three coupled first order differential equations". In: *Proceedings of the Royal Society of London B: Biological Sciences* 221.1222 (1984), pp. 87–102.

[28] Dong Liang Hu and Xian Bin Liu. "Delay-enhanced signal transmission in a coupled excitable system". In: *Neurocomputing* 135 (2014), pp. 268–272.

[29] Martin Tobias Huber and Hans Albert Braun. "Conductance versus current noise in a neuronal model for noisy subthreshold oscillations and related spike generation". In: *Biosystems* 89.1 (2007), pp. 38–43.

[30] Eugene M. Izhikevich. *Dynamical systems in neuroscience*. Cambridge, Massachusetts: The MIT press, 2007.

[31] Eugene M Izhikevich. "Neural excitability, spiking and bursting". In: *International Journal of Bifurcation and Chaos* 10.06 (2000), pp. 1171–1266.

[32] Eugene M Izhikevich. "Polychronization: computation with spikes". In: *Neural computation* 18.2 (2006), pp. 245–282.

[33] Eugene M Izhikevich. "Which model to use for cortical spiking neurons?" In: *IEEE transactions on neural networks* 15.5 (2004), pp. 1063–1070.

[34] Eugene M Izhikevich and Gerald M Edelman. "Large-scale model of mammalian thalamocortical systems". In: *Proceedings of the national academy of sciences* 105.9 (2008), pp. 3593–3598.

[35] Eugene M Izhikevich et al. "Simple model of spiking neurons". In: *IEEE Transactions on neural networks* 14.6 (2003), pp. 1569–1572.

[36] Eric Jones, Travis Oliphant, Pearu Peterson, et al. *SciPy: Open source scientific tools for Python*. 2001–. URL: http://www.scipy.org/.

[37] Sang-Yoon Kim and Woochang Lim. "Sparsely-synchronized brain rhythm in a small-world neural network". In: *Journal of the Korean Physical Society* 63.1 (2013), pp. 104–113.

[38] Jeffrey L Krichmar and Gerald M Edelman. "Brain-based devices for the study of nervous systems and the development of intelligent machines". In: *Artificial Life* 11.1-2 (2005), pp. 63–77.

[39] Chen Liu et al. "The effects of time delay on the stochastic resonance in feed-forward-loop neuronal network motifs". In: *Communications in Nonlinear Science and Numerical Simulation* 19.4 (2014), pp. 1088–1096.

[40] André Longtin. "Effects of noise on nonlinear dynamics". In: *Nonlinear Dynamics in Physiology and Medicine*. Springer, 2003, pp. 149–189.

[41] Jaime G Mancilia, Michael Fowler, and PHILIP S Ulinski. "Responses of regular spiking and fast spiking cells in turtle visual cortex to light flashes". In: *Visual neuroscience* 15.05 (1998), pp. 979–993.

[42] Henry Markram. "The blue brain project". In: *Nature Reviews Neuroscience* 7.2 (2006), pp. 153–160.

[43] KAC MARTIN. "A brief history of the feature detector". In: *Cerebral Cortex* 4.1 (1994), 1–7.

[44] SJ Martin, PD Grimwood, and RGM Morris. "Synaptic plasticity and memory: an evaluation of the hypothesis". In: *Annual review of neuroscience* 23.1 (2000), pp. 649–711.

[45] N Masuda and K Aihara. "Synchronization of pulse-coupled excitable neurons". In: *Physical Review E* 64.5, 1 (2001). ISSN: 1063-651X.

[46] Mark D McDonnell and Lawrence M Ward. "The benefits of noise in neural systems: bridging theory and experiment". In: *Nature Reviews Neuroscience* 12.7 (2011), pp. 415–426.

[47] Georgi S. Medvedev and Svitlana Zhuravytska. "Shaping bursting by electrical coupling and noise". In: *Biological Cybernetics* 106.2 (2012), 67–88. ISSN: 0340-1200. DOI: {10.1007/s00422-012-0481-y}.

[48] Mark N Miller, Benjamin W Okaty, and Sacha B Nelson. "Region-specific spike-frequency acceleration in layer 5 pyramidal neurons mediated by Kv1 subunits". In: *The Journal of Neuroscience* 28.51 (2008), pp. 13716–13726.

[49] Guowang Mu et al. "Human age estimation using bio-inspired features". In: *Computer Vision and Pattern Recognition, 2009. CVPR 2009. IEEE Conference on*. IEEE. 2009, pp. 112–119.

[50] *Neuroscience*. Sinauer Associates, 2001.

[51] Mark EJ Newman. "The structure and function of complex networks". In: *SIAM review* 45.2 (2003), pp. 167–256.

[52] Mark EJ Newman and Duncan J Watts. "Renormalization group analysis of the small-world network model". In: *Physics Letters A* 263.4 (1999), pp. 341–346.

[53] Mark EJ Newman and Duncan J Watts. "Scaling and percolation in the small-world network model". In: *Physical Review E* 60.6 (1999), p. 7332.

[54] Lionel G Nowak, Maria V Sanchez-Vives, and David A McCormick. "Influence of low and high frequency inputs on spike timing in visual cortical neurons." In: *Cerebral Cortex* 7.6 (1997), pp. 487–501.

[55] Lionel G Nowak et al. "Electrophysiological classes of cat primary visual cortical neurons in vivo as revealed by quantitative analyses". In: *Journal of neurophysiology* 89.3 (2003), pp. 1541–1566.

[56] Mahmut Ozer, Matjaž Perc, and Muhammet Uzuntarla. "Stochastic resonance on Newman–Watts networks of Hodgkin–Huxley neurons with local periodic driving". In: *Physics Letters A* 373.10 (2009), pp. 964–968.

[57] Satu Palva and J Matias Palva. "New vistas for α-frequency band oscillations". In: *Trends in neurosciences* 30.4 (2007), pp. 150–158.

[58] AJ Parker and WT Newsome. "Sense and the single neuron: Probing the physiology of perception". In: *Annual Review of Neuroscience* 21 (1998), 227–277.

[59] Ashok Patel and Bart Kosko. "Stochastic resonance in noisy spiking retinal and sensory neuron models". In: *Neural Networks* 18.5 (2005), pp. 467–478.

[60] RD Pinto et al. “Synchronous behavior of two coupled electronic neurons”. In: *Physical Review E* 62.2, B (2000), pp. 2644–2656. ISSN: 1063-651X.

[61] David Reid, Abir Jaafar Hussain, and Hissam Tawfik. “Spiking neural networks for financial data prediction”. In: *Neural Networks (IJCNN), The 2013 International Joint Conference on*. IEEE. 2013, pp. 1–10.

[62] Michael G. Rosenblum, Arkady S. Pikovsky, and Jürgen Kurths. “From Phase to Lag Synchronization in Coupled Chaotic Oscillators”. In: *Phys. Rev. Lett.* 78 (22 1997), pp. 4193–4196.

[63] E Salinas and TJ Sejnowski. “Correlated neuronal activity and the flow of neural information”. In: *Nature Reviews Neuroscience* 2.8 (2001), 539–550.

[64] Tim Sauer. “Reconstruction of dynamical systems from interspike intervals”. In: *Physical Review Letters* 72.24 (1994), p. 3811.

[65] William Erik Sherwood and John Guckenheimer. “Dissecting the phase response of a model bursting neuron”. In: *SIAM Journal on Applied Dynamical Systems* 9 (2010), pp. 659–703.

[66] Andrey Shilnikov and Marina Kolomiets. “Methods for the qualitative theory for the Hindmarsh-Rose mode: a case study”. In: *International Journal of bifurcation and chaos* 18.8 (2008), 2141–2168. ISSN: 0218-1274. DOI: {10.1142/S0218127408021634}.

[67] E Simonotto et al. “Visual perception of stochastic resonance”. In: *Physical Review Letters* 78.6 (1997), 1186–1189. ISSN: 0031-9007.

[68] Jesper Sjöström and Wulfram Gerstner. “Spike-timing dependent plasticity”. In: *Frontiers in Synaptic Neuroscience* (2011), pp. 35–44.

[69] Sen Song, Kenneth D Miller, and Larry F Abbott. “Competitive Hebbian learning through spike-timing-dependent synaptic plasticity”. In: *Nature neuroscience* 3.9 (2000), pp. 919–926.

[70] Michael Stich and Manuel G Velarde. “Interaction dynamics in small networks of nonlinear elements”. In: *Communications in Nonlinear Science and Numerical Simulation* 20.3 (2015), pp. 807–818.

[71] Harvey A Swadlow. “Monitoring the excitability of neocortical efferent neurons to direct activation by extracellular current pulses”. In: *Journal of neurophysiology* 68.2 (1992), pp. 605–619.

[72] Harvey A Swadlow. "Physiological properties of individual cerebral axons studied in vivo for as long as one year". In: *Journal of Neurophysiology* 54.5 (1985), pp. 1346–1362.

[73] Yang Tang et al. "Pinning noise-induced stochastic resonance". In: *Physical Review E* 87.6 (2013). ISSN: 1539-3755.

[74] Esther Verstraete et al. "Motor network degeneration in amyotrophic lateral sclerosis: a structural and functional connectivity study". In: *PloS one* 5.10 (2010), e13664.

[75] Stefan van der Walt, S. Chris Colbert, and Gael Varoquaux. "The NumPy Array: A Structure for Efficient Numerical Computation". In: *Computing in Science & Engineering* 13.2 (2011), 22–30. ISSN: 1521-9615.

[76] Yuqing Wang, ZD Wang, and W Wang. "Dynamical Behaviors of Periodically Forced Hindmarsh-Rose Neural Model: The Role of Excitability andIntrinsic'Stochastic Resonance". In: *Journal of the Physical Society of Japan* 69.1 (2000), pp. 276–283.

[77] Duncan J Watts and Steven H Strogatz. "Collective dynamics of 'small-world'networks". In: *nature* 393.6684 (1998), pp. 440–442.

[78] W. Wei, G. Perez, and H. Cerdeira. "Dynamical behaviour of the firings in a coupled neuronal system". In: *Physical Review E* 47 (1993), pp. 2893–2898.

[79] J. M. Wolfe, G. A. Alvaraz, and T. S. Horowitz. "Attention is Fast but Volition is Slow". In: *Nature* 406. (2000), 691.

[80] Jonathan R Wolpaw et al. "Brain–computer interfaces for communication and control". In: *Clinical neurophysiology* 113.6 (2002), pp. 767–791.

[81] Ying Wu et al. "Generalized synchronization induced by noise and parameter mismatching in Hindmarsh–Rose neurons". In: *Chaos, Solitons & Fractals* 23.5 (2005), pp. 1605–1611.

[82] Rui Yan, Meng Joo Er, and Huajin Tang. "An improvement on competitive neural networks applied to image segmentation". In: *Advances in Neural Networks-ISNN 2006*. Springer, 2006, pp. 498–503.

[83] Haitao Yu et al. "Chaotic phase synchronization in small-world networks of bursting neurons". In: *Chaos: An Interdisciplinary Journal of Nonlinear Science* 21.1 (2011), p. 013127.

[84] Hong-jie Yu and Jian-hua Peng. "Chaotic control of the Hindmarsh–Rose neuron model". In: *Acta Biophysica Sinica* 4 (2005), p. 006.

[85] Shan Yu et al. “A small world of neuronal synchrony”. In: *Cerebral cortex* 18.12 (2008), pp. 2891–2901.

[86] Sun Zhe and Ruggero Micheletto. “Noise influence on spike activation in a Hindmarsh–Rose small-world neural network”. In: *Journal of Physics A: Mathematical and Theoretical* 49.28 (2016), p. 285601.

[87] Yan Hong Zheng and Qi Shao Lu. “Spatiotemporal patterns and chaotic burst synchronization in a small-world neuronal network”. In: *Physica A: Statistical Mechanics and its Applications* 387.14 (2008), pp. 3719–3728.

[88] Eric A Zilli and Michael E Hasselmo. “Coupled noisy spiking neurons as velocity-controlled oscillators in a model of grid cell spatial firing”. In: *The Journal of neuroscience* 30.41 (2010), pp. 13850–13860.